ISRN LUTMDN/TMHP-15/5353-SE

ISSN 0282-1990

Preparation of electrospun fibres for solid oxide fuel cell anode

An exchange project at University of Electronic Science and Technology of China

Jonas Lindros

Thesis for the degree of Master of Science in Engineering
Division of Heat Transfer
Department of Energy Sciences
Faculty of Engineering | Lund University

Preparation of electrospun fibres for solid oxide fuel cell anode

An exchange project at University of Electronic Science and Technology of China

Jonas Lindros

June 2015, Lund

This degree project for the degree of Master of Science in Engineering has been conducted at the Division of Heat Transfer, Department of Energy Sciences, Faculty of Engineering, Lund University, and at University of Electronic Science and Technology of China in Chengdu, China.

Supervisor at the Division of Heat Transfer was Dr Martin Andersson
Supervisor at University of Electronic Science and Technology of China was Dr Li Tingshuai
Examiner at Lund University was Professor Bengt Sundén

The project was carried out in cooperation with the STINT-foundation who provided the funding for flight and accomodation.

Thesis for the Degree of Master of Science in Engineering

ISRN LUTMDN/TMHP-15/5353-SE

ISSN 0282-1990

Division of Heat Transfer
Department of Energy Sciences
Faculty of Engineering, Lund University
Box 118, 221 00 Lund
Sweden

www.energy.lth.se

Abstract

Climate change related issues make it urgent to develop alternative methods for producing electricity with low CO_2 emissions. Solid Oxide Fuel Cells (SOFC) have the potential of producing clean energy in stationary power generation with high efficiency. The problem is that to be more competitive the fabrication cost needs to be lowered. This can be done by for instance using less expensive raw materials. Todays prime anode material is a nickel/ yttria-stabilized zirconia cermet (Ni/YSZ). When manufacturing the anode material, the Ni is bound in nickel oxide (NiO) and the standard weight ratio used today is 50/50 for NiO/YSZ.

The purpose of the project in this thesis is to examine the possibility to decrease the Ni content in the anode material and still maintaining good electrochemical performance. To do this, four different anode materials with varying compositions of Ni/YSZ will be prepared. Three slurries containing NiO with ratio of 30-, 40- and 50 wt% NiO is to be prepared along with a pure YSZ slurry. These will then be used to fabricate fibres using electrospinning technique. Since Ni is one of the more expensive compounds in the anode, less use means lower fabrication cost. However, it is difficult to decrease the Ni-content and still have good cell performance. The foundation for good cell performance is to provide lots of triple phase boundaries, which are the sites where the electrochemical reactions of the anode occurs. The Ni works as the electron conductor in the anode and with interrupted Ni-chains the cell works poorly. The structural integrity of the anode is also affected by the Ni-content due to the difference in thermal expansion coefficient between Ni and YSZ.

Due to limited amount of time, successful fibres were only obtained for the 30 and 40 wt% NiO fibres. The 30 wt% NiO fibres were sintered at 400°C while the 40 wt% NiO fibres were sintered at 400, 450 and 500°C. The sintered fibres of the 30 wt% NiO had a dense structure but quite thin fibres. The 40 wt% NiO fibres had decreasing structural density with increased sintering temperature. These fibres were also relatively thin. It was concluded that another fabrication method might be more suitable, since the oxygen release during the reduction of the anode gives a great volume loss for the fibres and hence the structures might break. A more suitable fabrication method could be to prepare fibres with only 10% NiO and then add the rest by coating the fibres.

Keywords: *SOFC, anode material, Ni/YSZ, electrospinning, electrospun fibres, triple phase boundary*

Acknowledgements

This thesis includes 30 credits and is done over a full semester as the final part of the master program in Environmental Engineering at Lund University. The thesis has been performed as an exchange project between the Heat Transfer Division at Lund Institute of Technology, in collaboration with University of Electronic Science and Technology of China (UESTC) with funding from the STINT-foundation. Three months were spent at the department of Clean Energy Science and Materials at UESTC where all the experimental work were done.

I would like to express my greatest gratitude to my supervisor in China dr. Li Tingshuai for all the guidance during the project and for giving me an amazing experience in Chengdu. I would also like to thank my lab partners Linyun and Huiping for all the help with lab-related work and Huang Dengfeng for the SEM-images. Additionally, I thank everyone in UESTC for making my three months in China my best and most memorable part of my university time. I will always remember you!

Finally I would like to thank my supervisor Martin for all the support and encouragement through the semester.

2015-05-31

Jonas Lindros

Nomenclature and abbreviations

E	Nernst potential	V
E^0	Standard potential	V
F	Charge held by a mol of electrons	C mol^{-1}
FC	Fuel Cell	-
G	Gibbs free energy	J mol^{-1}
n_e	Number of charges	-
Ni	Nickel	-
NiO	Nickel oxide	-
PVP	Polyvinylpyrrolidone	C_6H_9NO
Q	Reaction quotient pressure	-
R	Gas constant	J K^{-1} mol^{-1}
SOFC	Solid oxide fuel cell	-
SEM	Scanning electron microscope	-
TPB	Triple phase boundary	-
W_e	Electrochemical work	J mol^{-1}
Y	Yttria	Y_2O_3
YSZ	Yttria-stabilized zirconia	-
Z	Zirconia	ZrO_2

Table of contents

1 Introduction

1.1 Background

Global warming and climate-change related issues put higher demands then ever on alternative and renewable energy sources to step forward and make a mark. The wind power industry and photovoltaic cells have, especially through the German *Energiewende* (The Economist, 2012), shown that a rapid expansion and large market shares for alternative energy sources is a real possibility. With the help of more research fuel cells could be next in line for rapid market development.

Fuel cell science and technology transcends across several disciplines such as electrochemistry, transport phenomena and materials science. The use this far has been limited to mainly space-related applications and auxiliary power units. However, with some breakthroughs it could grow rapidly in automotive usage and for solid oxide fuel cells (SOFC) within both stand-alone and combined heat and power generation.

The heritage of the fuel cell dates back to the 1800s when William R. Grove invented what he then called a ”gaseous voltaic battery”. It used platinum electrodes and sulphuric acid electrolyte and was powered by the reactants hydrogen and oxygen. The discovery was made when R. Grove reversed water electrolysis. The working principle of the fuel cell is unchanged since; “A fuel cell is an electrochemical device that continuously converts chemical energy into electric energy (and some heat) for as long as fuel and oxidant are supplied” (Hoogers, 2003).

The solid oxide fuel cell (SOFC) was developed in 1937 by Baur and Preis. The need for a more manageable electrolyte than the molten kind was a main driving force behind the development of SOFC:s. The solution was to be found in a solid compound developed by Wilhelm Nernst in 1899. Nernst had discovered that when heated up, mixed oxides had high conductivity. The solid compound that Baur and Preis used was a mixture of 85 mol% zicronia (ZrO_2) and 15 mol% yttrium (III) oxide (Y_2O_3) (Hoogers et al, 2003), (Kendal & Singhal, 2003).

The SOFC is a high temperature fuel cell. The typical operating temperature is in the range of 600-1000°C and allows for internal reforming of fuel. Hence, the SOFC is capable of working within a broader fuel spectrum than other types of fuel cells (Kreuer, 2013).

1.2 Motivation

The SOFC faces two main challenges for commercial success. The first one is the degradation issue for the cell and the second one is the manufacturing cost. One of the biggest costs in the

manufacturing process is the materials cost. In the anode, the nickel (Ni) is a relatively expensive material and the possibility of reducing the amount of Ni used can save money and make the SOFC more competitive (George & Bessetteb, 1998). Though, it is important to make sure that the cell performance still reaches a desirable level when trying to limit materials use.

Today, the prime anode material for SOFC is a double phase of nickel and yttria-stabilized zirconia (Ni/YSZ). The Ni is bound into nickel oxide (NiO) when preparing the anode material. This is then reduced down to pure Ni by applying fuel to the anode. The most common ratio between NiO and YSZ today is 1:1 (Pan, o.a., 2010). The Ni/YSZ cermet has been intensely analysed in terms of chemical stability and material fabrication. An important characteristic for cell performance is the structure and material composition of the anode. In the Ni-YSZ cermet the Ni act as catalyst and as an electron conductor while the YSZ is the foundation for dispersing the Ni preventing agglomeration. Additionally it transports the oxygen ions within the anode. It is important to establish an uninterrupted chain of Ni-Ni to diminish the electric resistance and to reach the percolation sill. One issue is the different thermal expansion coefficients of Ni and YSZ, which can cause structural instability when the cell is heated up (Li, Zhang, Liu, & Guo, 2010). The result is a limited range for the Ni-content and an importance for the process of manufacturing the Ni-YSZ framework to be precise.

1.3 Purpose, goals and limitations

The purpose of the project is to examine the possibility to decrease the Ni content in the anode material and still maintaining good electrochemical performance. The aim for this thesis is to create four anode frameworks with different compositions of the Ni-YSZ material. There are two part goals for this master thesis work:

1. The first one is to prepare our different slurries:
    - A pure YSZ slurry
    - YSZ+ 30 wt% NiO
    - YSZ+ 40 wt% NiO
    - YSZ+ 50 wt% NiO
2. The second goal is to create fibres from the slurries through a technique called electrospinning. After that the fibres will be sintered at high temperature.

The pure YSZ fibres will be coated with NiO after sintering and then the frameworks will be evaluated by testing the conductivity and porosity of the structures. However, since the time spent in China is limited these parts will be omitted from this thesis. Hence, this thesis is limited to just cover parts of the project. The project will continue when the author has left China.

1.4 Outline

The thesis is divided into chapters 2-7 with following content:

Chapter 2 describes how the fuel cell is built up and the thermodynamic mechanisms, chemical species involved and physical properties of the anode, cathode and electrolyte material as well as the stack design and operation process. The main emphasis are on the working principle and the anode microstructure since these are the most important parts for the thesis. Hence, the other parts describing the cathode, electrolyte, microstructure, cell- and stack design etc. are kept short.

Chapter 3 describes the methods used to conduct the experiments and the experimental setup. The main focus is on the steps performed in this thesis, but the evaluation and coating parts are also described.

Chapter 4 depicts the results gained from the experiments. SEM-images are depicted for every successfully sintered sample with four different magnifications.

Chapter 5 contains the discussion of the results as well as a section explaining the experimental difficulties that were encountered.

Chapter 6 inhibits the conclusion drawn from the work performed and some recommendations for future work.

Chapter 7 contains the learning and outcomes that have been gained from the exchange program.

2 Description of the Solid Oxide Fuel Cell

2.1 Introduction

The SOFC has a history of almost 80 years. The first SOFC was created by Baur and Preis in 1937. They first tried to use tubes made form ceramic materials including brickyard clay and two types of unglazed porcelain. The materials were tested at 1050°C and 1100°C but were deemed useless because of the high resistance. In a new attempt they switched the material to different mixtures containing zirconia. The best result was gained from the mixture containing zirconia and yttria. The composition, which was mentioned in the introduction, was 85 mol% zirconia and 15 mol% yttria and is called *Nernst-Mass* (Hoogers, 2003).

The SOFC has a great potential for stationary power production with high efficiencies compared to conventional power production methods. An Australian company holds the record of the highest efficiency as of today. For one of their home appliances, a cell operating on natural gas achieved an electrical efficiency of 60% (Ceramic Fuel Cells Limited, 2009). The SOFC is capable of working within a broad fuel spectrum due to its internal reforming abilities. The three main components that make up a SOFC are the anode (fuel electrode), the cathode (air electrode) and an electrolyte, which purely acts as an ion-conducting layer between the anode and cathode.

2.2 Working principle of the SOFC

The working mechanism for the SOFC is founded on oxygen anion transportation away from an O_2-rich environment at the cathode to the oxygen depleted environment at the anode. The outstanding feature of the SOFC compared to other FC:s is the dense electrolyte which electronically isolates the solid oxide but conducts oxygen anions (Kreuer, 2013).

The fuel and air are kept in physically and electronically separated chambers. The electrolyte act as the separating barrier and the entire cell is sealed to hinder fuel-air mixing. The electrolyte also provides the ion-bridge between the anode and cathode, while the electronic connection is via an external electric circuit. This connection is capitalised during operation when the electrolytic reduction of oxygen molecules into oxygen anions is creating an electron flow through the circuit. The anions then move from the cathode through the electrolyte to the anode oxidising the fuel, which liberates the electrons from the anions. Finally, the liberated electrons flow back through the circuit to the cathode. This current provides the useful work from the cell (Kreuer, 2013). A depiction of the SOFC is shown in figure 1 using H_2 as fuel.

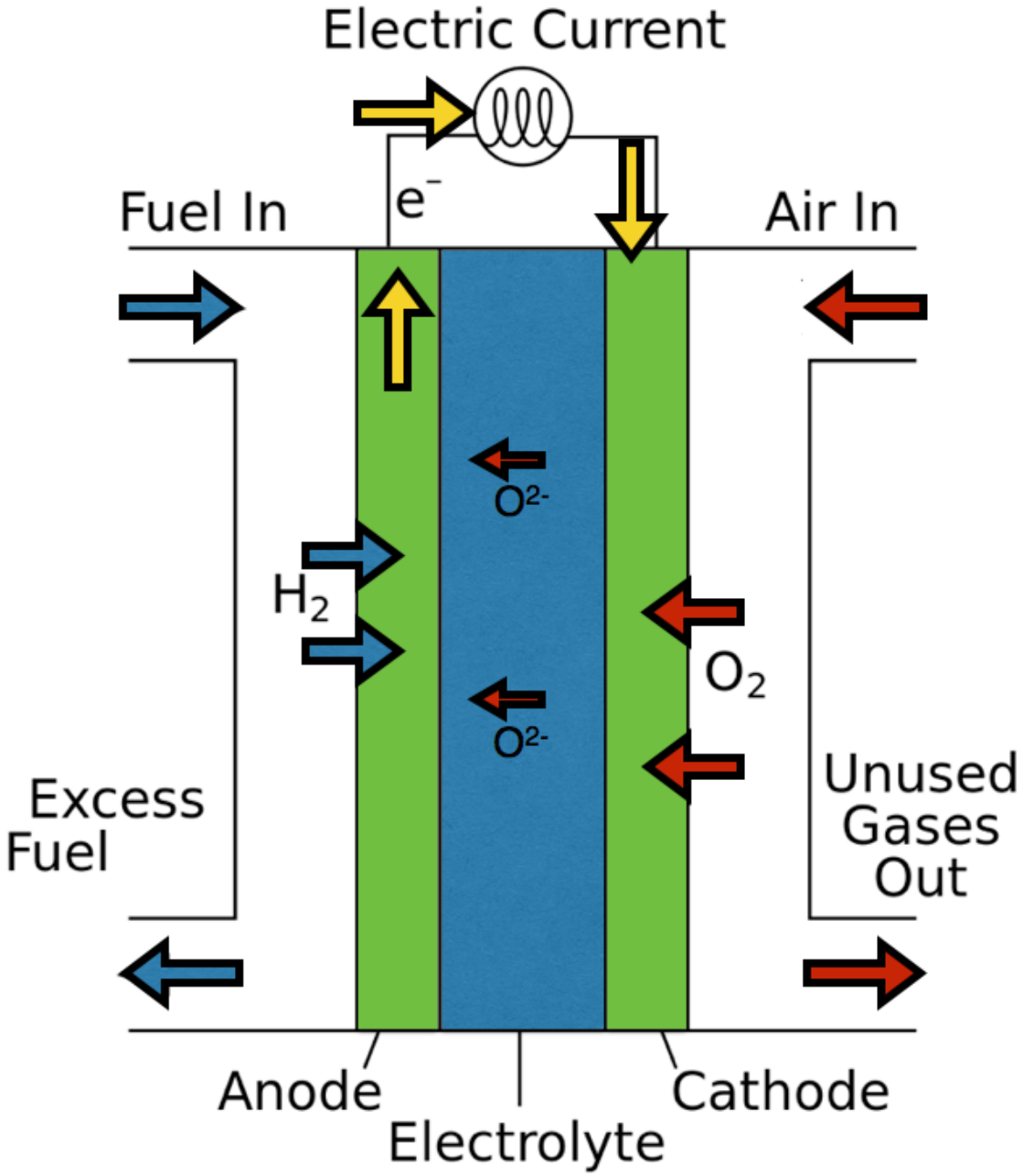

Figure 1 depicts a schematic of an SOFC using hydrogen as fuel (inspired by Sakurambo, Wikimedia Commons, 2015).

The fuel flows along the fuel electrode where it is diffused into the anode microstructure with a decreasing fuel concentration with decreased distance to the anode/electrolyte barrier. The microstructure of the anode is vital for how well the fuel is utilized. Another important factor is the fuel flow rate. With a too high flow rate the fuel ability to diffuse into the microstructure is reduced. The same principle goes for the air electrode side where the oxygen diffuses into the microstructure and is reduced to oxygen anions. The differences of the structures of the electrodes compared to the electrolyte are visualized in figure 2 below. The dark electrolyte barrier can be seen in between the two porous electrode structures. The left

side of the picture shows the air electrode and the fuel electrode can be seen on the right side along with the support structure.

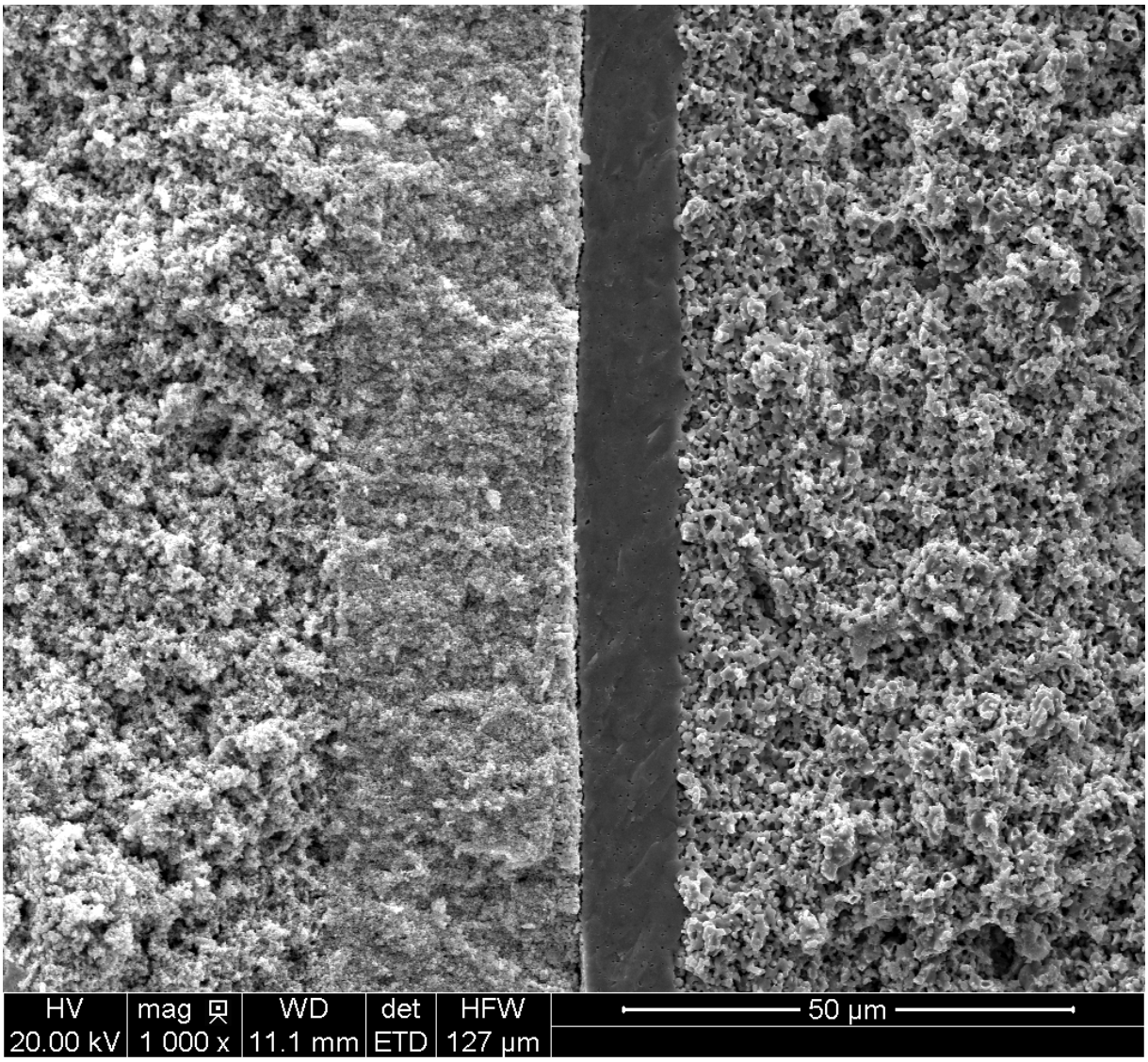

Figure 2 shows an SEM-image of the anode, cathode and electrolyte magnified a 1000 times (Reproduced with permission from Li Tingshuai).

2.3 Chemical reactions and thermodynamics of the cell

The maximal energy that can be extracted from a system is related to the change in Gibbs Energy

$$\boldsymbol{\Delta G = \delta W_e} \qquad \textbf{Eq. 2-1}$$

where W_e is the electrochemical work. This can be rewritten by rewriting the work term:

$$\boldsymbol{W_e = n_e F E} \qquad \textbf{Eq. 2-2}$$

The n_e is the number of transferred electrical charges in a reaction, F is charge held by a mol of electrons or protons. The last term E is the voltage difference between the electrodes (Suzuki, Hasan, Funahashi, Yamaguchi, Fujishiro, & Awano, 2009). Given a negative sign, the work equals the change in Gibbs energy:

$$\boldsymbol{\Delta G = -n_e F E} \qquad \textbf{Eq. 2-3}$$

Equation 2-3 also applies for the standard potential E^0, defined by the standard Gibbs energy:

$$\boldsymbol{\Delta G^0 = -n_e F E^0} \qquad \textbf{Eq. 2-4}$$

Another expression for the change in Gibbs free energy for gas mixtures involving the gas constant R, temperature T and the general reaction quotient for the pressures Q, is presented in equation 2-5 (Suzuki, Hasan, Funahashi, Yamaguchi, Fujishiro, & Awano, 2009).

$$\boldsymbol{\Delta G = \Delta G^0 + RT ln\, Q} \qquad \textbf{Eq. 2-5}$$

The voltage level of the cell E, can now be expressed by combining equation 2-3 and 2-5 into one.

$$\boldsymbol{E = -\frac{\Delta G^0}{n_e F} - \frac{RT}{n_e F} \ln Q} \qquad \textbf{Eq. 2-6}$$

By inserting equation 2-4 into 2-6 a general formula for calculating the theoretical open circuit potentials is reached called Nernst Equation:

$$\boldsymbol{E = E^0 - \frac{RT}{n_e F} ln\, Q} \qquad \textbf{Eq. 2-7}$$

2.3.1 Electrode reactions and reforming

To gain the maximum amount of energy it is vital that a total oxidation of the fuel is reached. Only then, it is possible to harvest all the potential chemical energy. The complete oxidation of hydrogen and methane are depicted in equation 2-8 and 2-9. These are the reactions that ideally occur at the anode.

$$\mathbf{H_2 + O^{2-} \rightarrow H_2O + 2e^-} \qquad \textbf{Eq. 2-8}$$

$$\mathbf{CH_4 + 4O^{2-} \rightarrow CO_2 + 2H_2O + 8e^-} \qquad \textbf{Eq. 2-9}$$

However, especially in the case of methane, the pathway to full oxidation is not a smooth ride and there is no guaranty that the end product will be carbon dioxide, water and electrons. There are many possible pathways like full oxidation (eq. 2-9), partial oxidation to CO and H_20 (eq. 2-10), steam or dry reforming with H_2O (eq. 2-11) and CO_2 (eq. 2-12) from

previously reacted CH_4 and a possibility of forming graphitic carbon and hydrogen gas (eq. 2-13).

$$\mathbf{CH_4 + 3O^{2-} \rightarrow CO + 2H_2O + 6e^-} \quad \textbf{Eq. 2-10}$$

$$\mathbf{CH_4 + H_2O \rightarrow CO + 2H_2} \quad \textbf{Eq. 2-11}$$

$$\mathbf{CH_4 + CO_2 \rightarrow 2CO + 2H_2} \quad \textbf{Eq. 2-12}$$

$$\mathbf{CH_4 \rightarrow C + 2H_2} \quad \textbf{Eq. 2-13}$$

This complexity increases with the length of the carbon chain for hydrocarbons. One of the main advantages of the SOFC is that its high operating temperature allows for internal reforming, either through steam reforming (eq. 2-11) or dry reforming (eq. 2-12). These reactions are both endothermic and that is why they need a very high temperature to occur. The benefit of reforming is that the products of the reforming are more easily oxidised than the original hydrocarbon, and the possibility of carbon deposition decreases when reformed with the right agent (Wongchanapai, Iwai, Saito, & Yoshida, 2012). O^{2-}

At the cathode, oxygen is reduced into oxide ions.

$$\mathbf{O_2 + 4e^- = 2O^{2-}} \quad \textbf{Eq. 2-14}$$

2.4 Anode material and microstructure

The requirements for the anode material can be expressed in three clear requirements. Firstly, the oxygen anions must be able to be transported to the reaction site. This demands great oxygen anion conductivity. Secondly, the anode is required to electro catalytically promote the desired oxidation of the fuel (Li & Xia, 2004). Finally it must possess proper electronic conductivity to enable electron transport from the reaction site to the dedicated current wire. Besides these basic requirements there are issues of porosity and tortuosity for gas diffusion, compatibility and stability during cell operation, structural stability and impurity sensibility (Kreuer, 2013). Hence, the manufacturing of anode material faces great challenges.

The most common material used for anode manufacturing is a Ni/YSZ cermet. As mentioned in the introduction the Ni provides the electron conductivity and oxidation surface for the fuel while the YSZ provides the ionic conductivity.

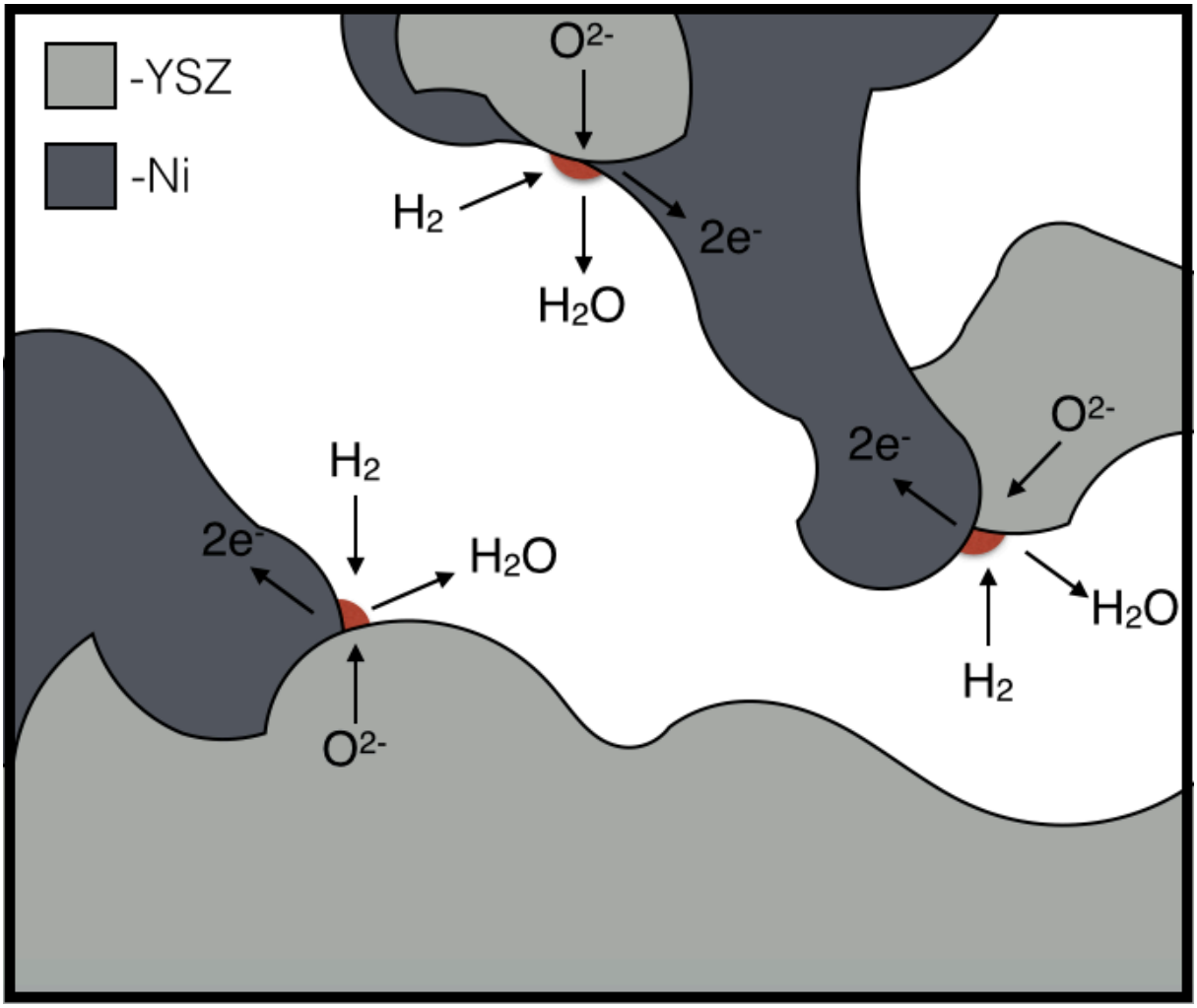

Figure 3 visualises the structure of the anode material and the reactions occurring. Inspired by (Kreuer, 2013).

The reactions occurring at the different parts of the anode is depicted in figure 2. The fuel shown here is H_2 with the reaction from equation 2-8. The requirement for a reaction to occur is a three surface border between the interfaces of Ni and YSZ and the gas phase. This is known as a ***triple phase boundary*** (TPB). A poorly manufactured anode will struggle to perform well since too few reactions will take place. When designing the anode it is vital to provide lots of TPB:s to have good cell performance. Terms such as porosity, Ni/YSZ particle size and interconnectivity are the key to this (van den Bossche & McIntosh, 2013).

The porosity and tortuosity of the structure is vital to provide good gas diffusion so that the fuel can reach all the potential reaction spots. Finger like structures provides hundreds of micro-channels in the asymmetric anode material for the mass transport of gas. However, the cavities, though useful for gas diffusion, can cause difficulties in the electrolyte film. Macro-pores in the top and bottom of surfaces of the electrode substrate increase the difficulties of creating a defect-free large area dense thin electrolyte film (Chen, Bunch, Li, Mao, & Chen, 2012).

The porosity and tortuosity of the structure is important not only for fuel but also for the removal of water steam during high operating temperatures. Insufficient removal of steam can lead to Ni oxidation and agglomeration, which affects the performance (Chen, Bunch, Li, Mao, & Chen, 2012).

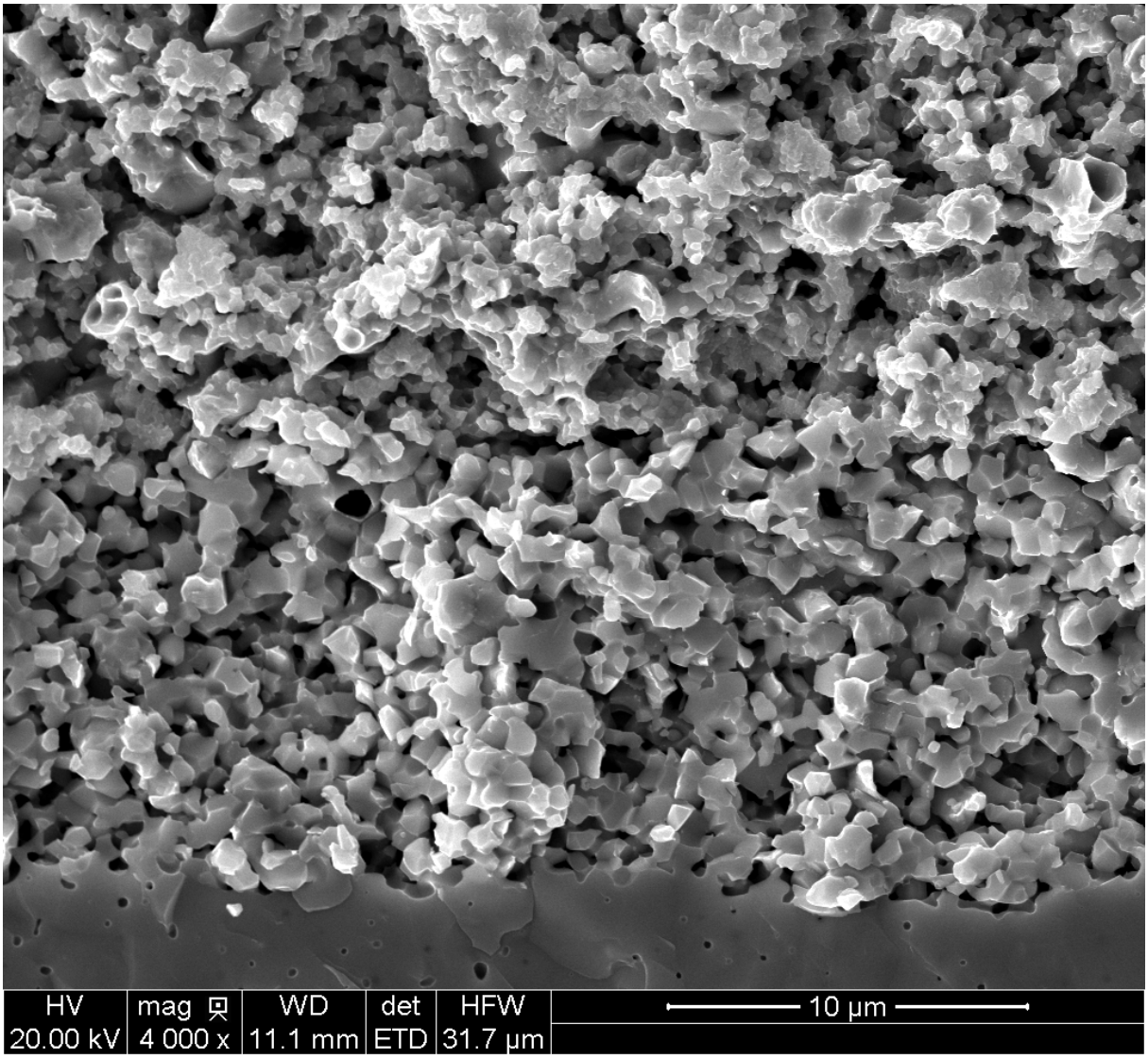

Figure 4 depicting a SEM-image of the porous structure of an anode fabricated by freeze-tape casting method (Reproduced with permission from Li Tingshuai).

The commonly used anode material YSZ is a ceramic made out of zirconium dioxide or as it is commonly called Zirconia (ZrO_2) and yttrium (III) oxide or Yttria (Y_2O_3). It has some properties, which makes it suitable for use in a SOFC-anode. It has a very high melting point, and is thusly ready to deal with the high temperatures of the cell. Additionally, it has good oxide ion conductivity when heated up; hence it is suitable for using as the ion conductor of the anode material.

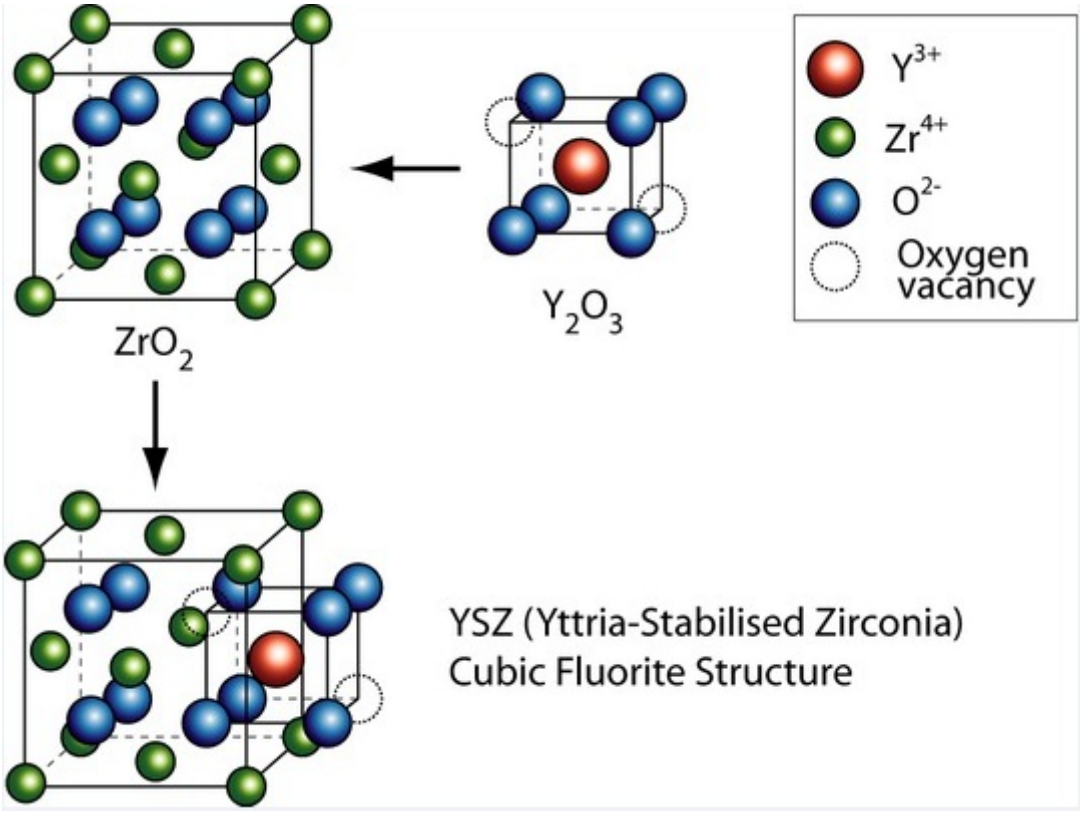

Figure 5 visualising the structure of zirconia, yttria and YSZ (University of Cambridge, Wikimedia Commons, 2015).

The zirconia experiences three different polymorphs. At room temperature, it has a monoclinic structure, which leaves little oxygen vacancy. At temperatures above 1170°C it changes into a tetragonal structure and above 2370°C it shapes into a cubic fluorite structure. Both of these shapes have a higher oxygen vacancy than the monoclinic crystal structure. When Yttria is added, the tetragonal and cubic fluorite structures are stabilised down to room temperature (Kendal & Singhal, 2003). The cubic fluorite structure is depicted in figure 3. The mol percentage of yttria is dependent on the stoichiometric mix between the yttria containing compound and the zirconium containing compound when manufacturing the YSZ but a common number is 8 mol% (Zhao, Xie, & Wang, 2013).

For the cell to perform well, the electrons must be able to be transported away from the anode to keep charge neutrality. Thus, it is important that the Ni-chain is uninterrupted. Just the slightest interruption can affect cell performance (Li, Wang, He, Chen, & Xu, 2010). The normal way to fabricate a nickel cermet anode is by sintering after slurry coating (Kreuer, 2013). The Ni is bond into Nickel oxide (NiO) when manufacturing the anode material. After preparing the anode material the NiO is reduced into pure Ni by the fuel when operating the cell. The weight ratio of NiO/YSZ can be altered but the minimum threshold today is 44.38 wt% of Ni. The standard weight ratio used today is 1:1 for NiO/YSZ (Pan, o.a., 2010). An issue regarding the Ni-content is that the electron transport requires a continuous Ni-chain, while the structural integrity of the anode suffers when the Ni-content is too high. This is due to the difference in thermal expansion coefficient (TEC) between the Ni and the YSZ (Li,

Zhang, Liu, & Guo, 2010). Thus, finding ways to decrease Ni content without lowering performance is desirable.

2.5 Cathode material and microstructure.

The important characteristics for the cathode include high electric conductivity, high oxygen reduction activity and compatibility with other cell material. In the early history of the SOFC, platinum was used as the cathode material. However the expensiveness of the platinum makes it non-useful in cost-effective SOFC:s and thus it is not used anymore as cathode material. Today, the dominating cathode material for high temperature SOFC:s (operating temperature of 1000°C) is lanthanum manganite-based material. For intermediate SOFC:s (operating temperature down to 700°C) a composite of strontium doped lanthanum manganite (LSM) and YSZ is used. The surface area, microstructure and the porosity, determines the performance of the cathode. Hence the fabricating method for the cathode is important (Kendal & Singhal, 2003).

2.6 Electrolyte

The requirements for the electrolyte material in a SOFC are to have low electron conductivity, good stability in both reducing and oxidising environment and acceptable oxide ion conductivity at the operating temperature. Additionally the material must be able to be formed into a strong, thin film with no gas leaks. YSZ is the most commonly used electrolyte material. There are other materials that have higher oxide ion conductivity like Scandia-doped zirconia but due to the expensive nature of Scandia this is not widely used (Kendal & Singhal, 2003).

2.7 Cell and stack design

There are many ways to design a cell and the cell stack. The earliest designs were in the form of discs. Since the 60:s though, the main focus has been on tubular and on planar designs. Under typical operating conditions the production of a single cell is very low. To obtain high power output it is a necessity to stack many cells together. This is done by using interconnect material which often also fills other functions like provide channels for air and fuel flow and seal the cell (Kendal & Singhal, 2003).

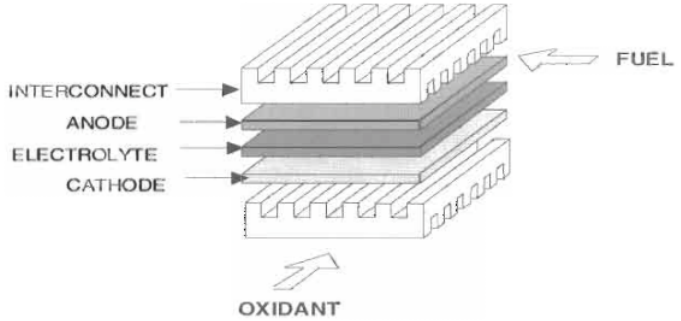

Figure 6 depicting a SOFC with interconnects (Kendal & Singhal, 2003).

2.8 Start-up, operating process and combined systems

The typical operating temperatures for the SOFC is between 600 and 1000°C (Kunze, Paschos, & Stimming, 2013). This gives many advantages but also drawbacks. The ramp-up time increases with rising operating temperature (Chen, Bunch, Li, Mao, & Chen, 2012). For experimental setup the SOFC is usually put in a furnace to reach the operating temperature. In a commercial cell, this setup would not be feasible since there is a need for waste heat recovery. In fact, in a commercial SOFC the fuel cell is only a small part of the whole fuel cell reactor. The rest consists of thermal insulation, heat exchangers for waste heat recovery, pipe-works, start-up heater and fuel processor.

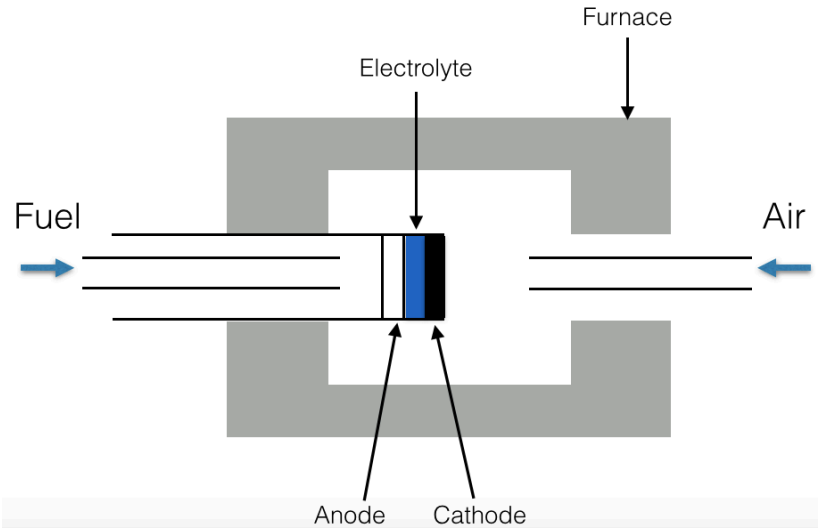

Figure 7 depict an experimental setup for SOFC. Inspired by (Kendal & Singhal, 2003).

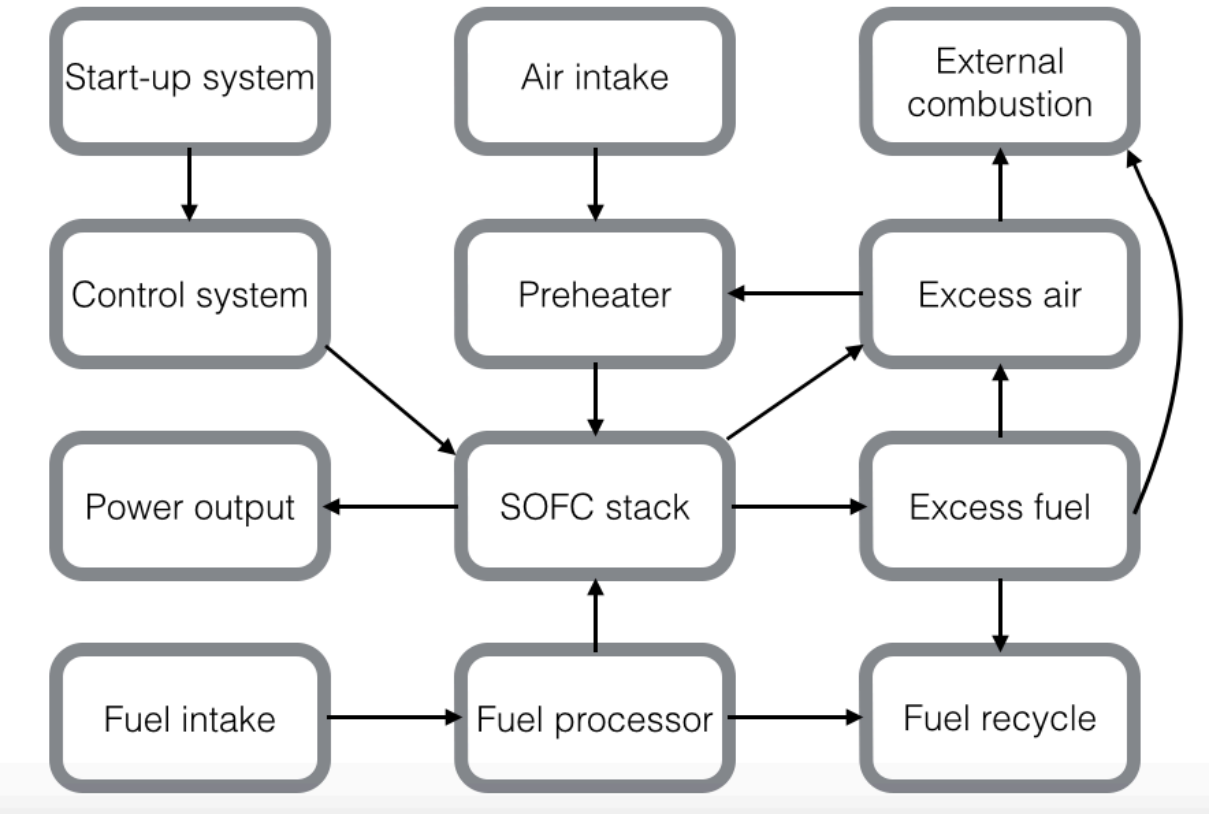

Figure 8 shows the process scheme for a possible commercial SOFC setup. Inspired by (Kendal & Singhal, 2003).

When comparing figure 7 and 8 it is evident how much simpler the experimental setup is. The commercial SOFC can also be combined with either steam cycle with boiler and steam turbine, or with a gas turbine. This increases the efficiency for the total system (Kreuer, 2013). In a combined system with a SOFC and a gas turbine, external combustion is used in combination with burning the fuel that was not utilized by the fuel cell. In the combined system of a steam cycle and a SOFC the waste heat is utilized together with the excess fuel that has passed through the cell.

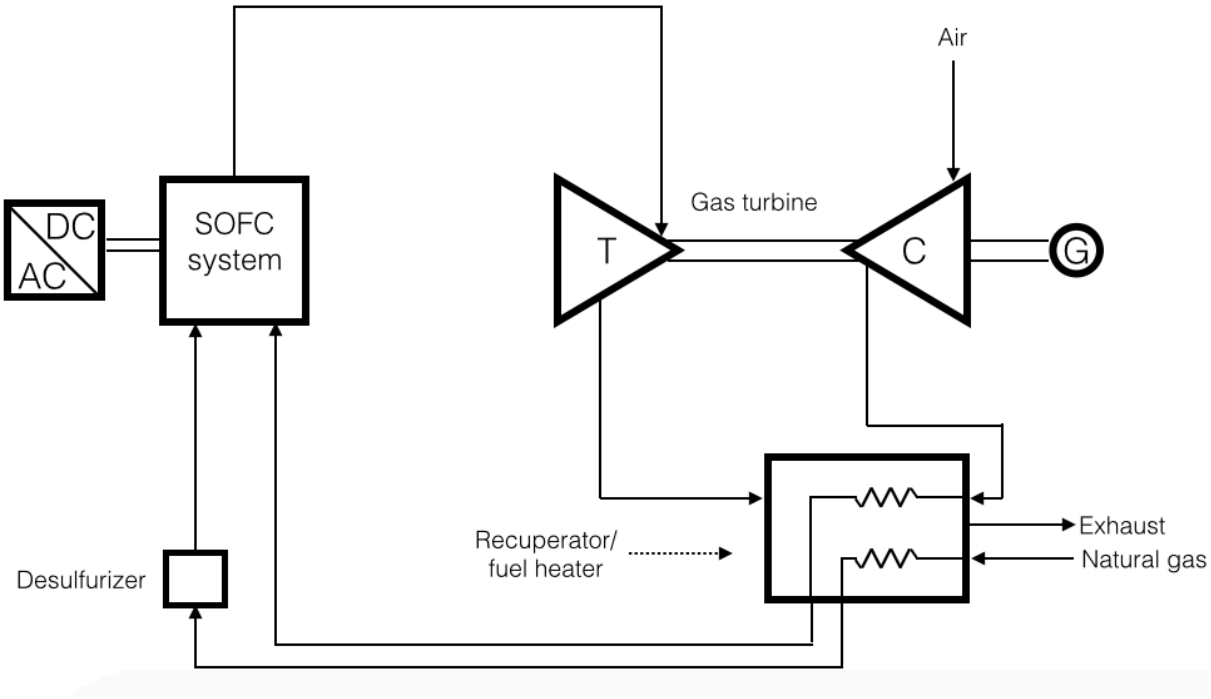

Figure 9 depicts a system that combines a SOFC with a gas turbine.

2.9 Main issues for competitiveness

2.9.1 Degradation processes

One of the greatest challenges for the SOFC is the different degradation process that occurs during operation. The combination of high operating temperatures and a variety of chemical species together with the complex structure of the anode cermet presents great challenges to avoid depositions and other processes, which lowers the efficiency. Two of the most thoroughly examined impurity and degradation related issues are listed below.

2.9.1.1 Carbon deposition

One of the outstanding features of the SOFC is its ability to run on multiple fuels. However, there are issues with using hydrocarbons to power the cell. The carbon can deposit on the anode, which changes the microstructure of the Ni-cermet. The deposited carbon acts as a catalyst for further carbon deposition. Eventually, this can lead to a blockage of the fuel flow in the pores of the anode. The possibility of carbon deposition from hydrocarbons increases with carbon number. This is due to the decrease in decomposition temperature for increasing carbon number (Kreuer, 2013).

2.9.1.2 Sulfur poisoning

Sulphur contaminants are dependent of the configuration of the SOFC stack. For some stationary applications a desulphurization process is put in front of the reforming process.

Hence there is no expectation of sulphur poisoning. Performance degradation for the anode originates from hydrogen sulphur reacting with oxide ions.

$$\mathbf{H_2S\,(g) + \ 0.5\ O^{2-} \rightarrow S(on\ Ni) + \ H_2O + 2e^-} \qquad \textbf{Eq. 2-15}$$

This can slowly degrade the cell performance with sulphur being accumulated inside nickel particles due to sulphur dissolution and diffusion (Yokokawa & Horita, 2012).

2.9.2 Cost issues

The costs along with the degradation process are the two main issues for making the SOFC competitive. Cost, performance and degradation are closely linked together and affect each other. The costs consist of three parts; material cost, cell/fabrication cost and system cost. When changing material to decrease degradation the usual effect is a cost increase due to additional treatments and other material processes. Hence a trade-off has to be made between durability and cost. To evaluate and cut the costs of the SOFC five parts are taken into consideration (George & Bessetteb, 1998):

1. The recognition of high cost elements. For example, the Ni in the anode is an expensive material along with the Y in YSZ and La in cathodes or interconnects. It is therefore vital to minimize the use of such elements and find appropriate fabrication methods.
2. Low-cost materials when suitable. The impurity issue can be a limiting factor here.
3. Reduction of the number of components in multiple stack-units.
4. Minimization of losses during fabrication
5. Automated fabrication.

3 Methodology, experimental setup and equipment

3.1 Introduction

This thesis will be based upon the preparation of four different anode-materials for a SOFC. To begin with, anode materials were prepared by mixing four different slurries:

- A pure YSZ slurry
- YSZ+ 30 wt% NiO
- YSZ+ 40 wt% NiO
- YSZ+ 50 wt% NiO

The slurries were then used to form anode structures through a technique called electrospinning. After the electrospinning, the slurries had transformed into long and thin fibres. These fibres were sintered at high temperature. This is how far the thesis will cover since the time in China was limited. Since the pure YSZ fibres lack an electron conductor it will be coated with NiO after the sintering. The final step is to evaluate the properties of the fibres. This will be done by measuring the electrical resistance through electrochemical impedance spectroscopy (EIS) and by measuring the porosity of the structure.

Note! *Since coating and evaluation part will be done after the author has returned from China; these parts will not be covered deeply in the methodology part.*

3.2 The slurry mixing

Four different slurries were prepared. For the three slurries containing NiO, the chemicals used were glycine (NH_2CH_2COOH), zirconium (IV) oxynitrate hydrate ($ZrO(NH_3)_2{*}xH_2O$), yttrium nitrate hexahydrate ($Y(NO_3)_3{*}6H_2O$) and nickel nitrate hexahydrate ($Ni(NO_3)_2{*}6H_2O$). The pure YSZ-slurry contained no nickel nitrate hexahydrate. The YSZ was mixed with a ratio of 8 mol% of Y.

Table 1 describes the formulas and molecular weight of the four different substances used to make the slurries.

Substance	Zirconium (IV) oxynitrate hydrate	Yttrium nitrate hexahydrate	Nickel nitrate hexahydrate	Glycine
Chemical formula	$ZrO(NH_3)_2{*}H_2O$	$Y(NO_3)_3{*}6H_2O$	$Ni(NO_3)_2{*}6H_2O$	NH_2CH_2COOH
Mol. Weight (g/mol)	231.23	383.01	290.79	75.07

3.2.1 Weight calculation for Ni

In order to get the correct mass and mol substances of the YSZ and NiO slurries it is important to first calculate the correct masses. The general formula used to gain the correct amounts are expressed as:

$$\boldsymbol{Wt}\%\ \mathbf{NiO} = \frac{\boldsymbol{Wt}\ \mathbf{NiO}}{\boldsymbol{Wt}\ \mathbf{NiO} + \boldsymbol{Wt}\ \mathbf{ZrO_2} + \boldsymbol{Wt}\ \mathbf{Y_2O_3}} \qquad \textbf{Eq. 3-1}$$

To retrieve a usable equation for calculating the correct amount of NiO equation 3-1 is developed by replacing the mass through multiplying the amount of substance n with the molar mass M.

$$\boldsymbol{Wt}\%\ \boldsymbol{NiO} = \frac{\boldsymbol{n}_{\mathbf{NiO}} \cdot \boldsymbol{M}_{\mathbf{NiO}}}{\boldsymbol{n}_{\mathbf{NiO}} \cdot \boldsymbol{M}_{\mathbf{NiO}} + \boldsymbol{n}_{\mathbf{ZrO_2}} \cdot \boldsymbol{M}_{\mathbf{ZrO_2}} + \boldsymbol{n}_{\mathbf{Y_2O_3}} \cdot \boldsymbol{M}_{\mathbf{Y_2O_3}}} \qquad \textbf{Eq. 3-2}$$

Since the substance amounts of ZrO_2 and Y_2O_3 are set at fixed levels equation 3-2 can be rewritten to express the amount of NiO.

$$\boldsymbol{n}_{\mathbf{NiO}} = \boldsymbol{Wt}\%\ \mathbf{NiO}\ \frac{\boldsymbol{n}_{\boldsymbol{ZrO_2}} \cdot \boldsymbol{M}_{\boldsymbol{ZrO_2}} + \boldsymbol{n}_{\boldsymbol{Y_2O_3}} \cdot \boldsymbol{M}_{\boldsymbol{Y_2O_3}}}{\boldsymbol{M}_{\mathbf{NiO}}(\mathbf{1} - \boldsymbol{Wt}\%\ \mathbf{NiO})} \qquad \textbf{Eq. 3-3}$$

The calculated amount of substance of NiO corresponds to the amount of nickel nitrate hexahydrate to be added to the slurry mix.

$$\boldsymbol{n}_{\mathbf{NiO}} = \boldsymbol{n}_{\boldsymbol{Ni(NO_3)_2 \cdot 6H_2O}} \qquad \textbf{Eq. 3-4}$$

Table 2 depicts the amount of substance to be added to the slurry mix.

Substance	Zirconium (IV) oxynitrate hydrate	Yttrium nitrate hexahydrate	Nickel nitrate hexahydrate
30 Wt % NiO (g)	2.12	0.31	0.67
40 Wt % NiO (g)	2.12	0.31	0.79
50 Wt % NiO (g)	2.12	0.31	0.93
Pure YSZ (g)	2.12	0.31	-

3.2.2 Weight calculation for glycine

The glycine works as an oxidizing agent for the zirconium, yttrium and nickel. The nitrate is replaced by oxygen to form zirconia, yttria and nickel oxide.

$$9ZrO(NH_3)_2 + 10C_2H_5NO_2 \rightarrow 9ZrO_2 + 14N_2 + 20CO_2 + 25H_2O \quad \text{Eq. 3-5}$$

$$6Y(NH_3)_3 + 10C_2H_5NO_2 \rightarrow 3Y_2O_3 + 14N_2 + 20CO_2 + 25H_2O \quad \text{Eq. 3-6}$$

$$9Ni(NH_3)_2 + 10C_2H_5NO_2 \rightarrow 9NiO + 14N_2 + 20CO_2 + 25H_2O \quad \text{Eq. 3-7}$$

Since the amount of the zirconium- and the yttrium containing compounds are known and the NiO amount has been calculated, equation 3-5 to 3-7 can be used for calculating the mass of glycine needed.

Table 3 shows the mass of glycine for the different slurries

Substance	Glycine
30 Wt % NiO (g)	1.04
40 Wt % NiO (g)	1.09
50 Wt % NiO (g)	1.12
Pure YSZ (g)	1.00

3.2.3 Mixing method

For the slurries containing Ni, the four chemicals with masses according to table 2 and table 3 were solved one by one in 10 ml of distilled water with continuous stirring. When the solution had become clear, polyvinylpyrrolidone (PVP, $(C_6H_9NO)_n$) was added to increase the viscosity, which is a necessity to perform the electrospinning. The mass of PVP for the different slurries is depicted in table 4. The PVP was added in small amounts of 0.25 g to ensure the right thickness was reached. When all the PVP had dissolved the slurries were ready for the electrospinning process.

Figure 10 depicts the mixed slurries for the 40- and 50 wt% YSZ-NiO slurries. The green colour originates from the $Ni(NH_3)_2$ crystals.

Table 4 shows the mass of PVP added to the slurries.

Substance	PVP
30 Wt % NiO (g)	1.50
40 Wt % NiO (g)	1.50
50 Wt % NiO (g)	1.50
Pure YSZ (g)	1.50

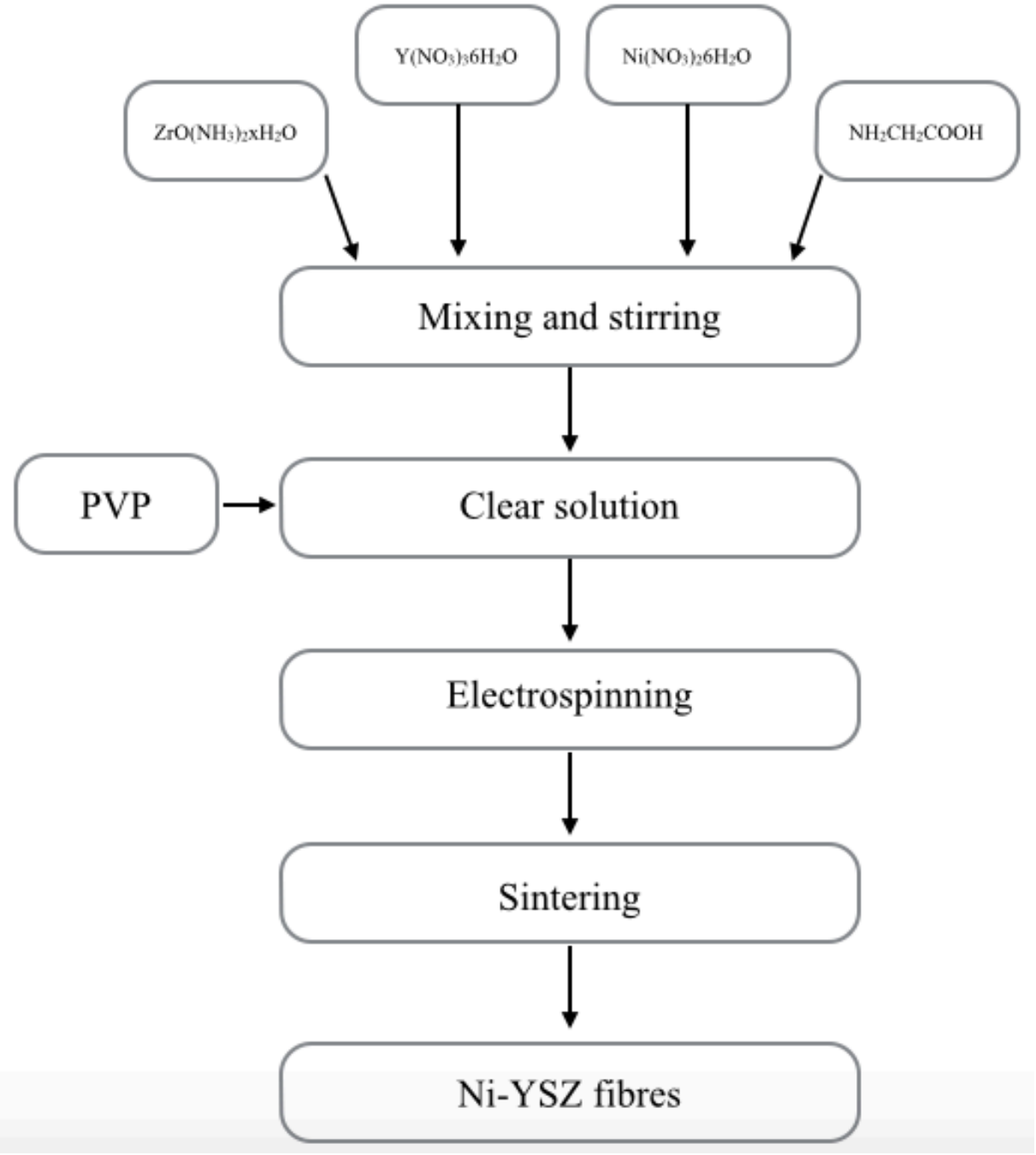

Figure 11 depict an overview of the experimental method for the Ni-containing anode material.

The pure YSZ slurry was mixed in the same way as the other slurries except there were no Ni-containing chemical added. The Ni was to be added in a later stage when the fibres had been sintered.

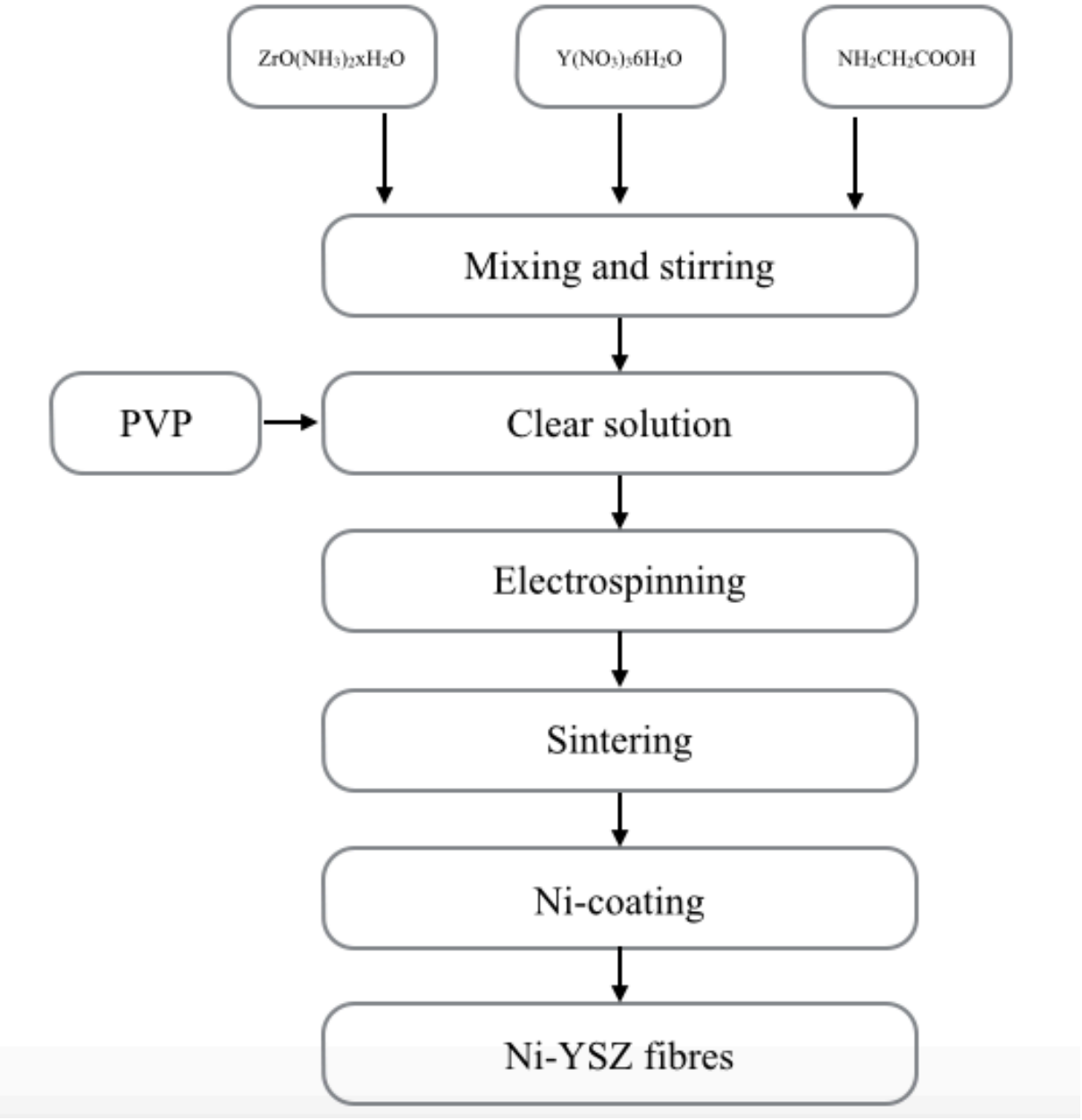

Figure 12 visualize the experimental work process step by step for the pure YSZ slurry.

3.3 Electrospinning

3.3.1 Background and theory

The electrospinning technique dates back to a patent from 1934. The patent regarded a device that used electrostatic repulsions between surface charges to produce polymer filaments. The technique was then known as electrostatic spinning. However, until the early 1990:s there were very few publications on the subject. During this period, several research groups revitalized interest in the technique by demonstrating thin fibres from a vast diversity of

organic polymers. This was also the time when the name electrospinning was introduced (Li & Xia, 2004).

The basic setup for electrospinning consists of three major parts: a spinneret (a metallic needle), a high voltage source and a collector. The spinneret connects to a syringe, which supplies the material for the electrospinning. The syringe pump enables a constant and controllable flow rate of solution through the spinneret. A high voltage is then applied to the drop of solution at the nozzle of the spinneret. The drop of the solution at the tip of the nozzle of the spinneret becomes electrified and charges are evenly distributed over the surface (Li & Xia, 2004).

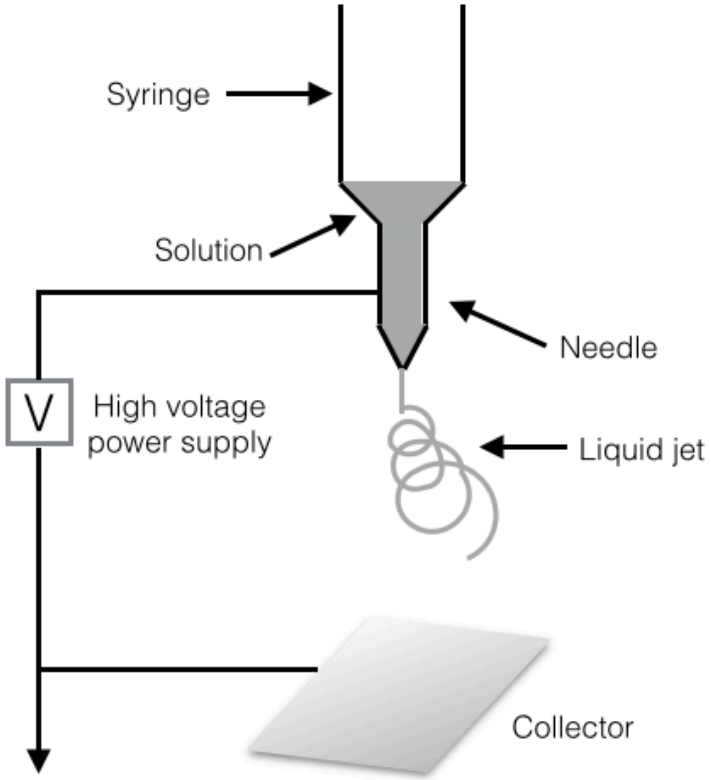

Figure 13 visualises the electrospinning process.

Two major types of electrostatic forces affect the droplet: the coulombic force exerted by the external electrical field and the electrostatic repulsion between the surface charges. This leads to a distortion of the liquid droplet that is formed into a conical shape. The shape is known as a Taylor cone. When the strength of the electrical field reaches a threshold limit, the electrostatic forces overcome the surface tension of the polymer solution and force an ejection of a liquid jet from the nozzle. The jet is stretched and whipped into a long and thin thread. The diameter of the jet can be reduced from hundreds of micrometres to as small as tens of nanometres. The charged fibre is attracted to the collector where it deposits. The fibres are often randomly dispersed on the collector to form a non-woven mat. There are other methods to collect the fibres. It is common to use a rotating drum to collect the fibres. Since the setup for electrospinning is simple it can easily be modified in many ways (Li & Xia, 2004).

The shape and size of the electrospun fibres depend on a lot of different properties of the fluid including the viscosity, elasticity, electrical conductivity, the polarity and surface tension of the solvent. The operational conditions are also important factors for determining the fibre morphology such as strength of the applied electrical field, the distance between the spinneret and collector and the feeding rate of the solution. External factors like humidity and temperature of the surroundings can also affect the result. In general, the cross section of the electrospun fibres is circular. The electrospinning process is a low-productivity process with feeding rates usually below 1 ml/h. If the solution is fed to fast the fibres will be too thick. Another important factor for thickness is the concentration of the substance. A higher concentration will give thicker fibres (Li & Xia, 2004).

3.3.2 Setup

The experimental setup used in the lab contained a high voltage power supply, an electrically insulated box coated in plastic wrapping, two electrodes, and a stand with holding device for the syringe. The collector plate was fixed to a piece of aluminium foil, which was connected to one of the electrodes. The collector plate is a piece of glass that has a conducting side and a non-conducting side. The glass plate was placed so the conducting side was turned up facing the needle. This setup lacked a syringe pump and thus was only relying on gravity to feed the solution. Hence the only way to control the flow was through the viscosity of the solution.

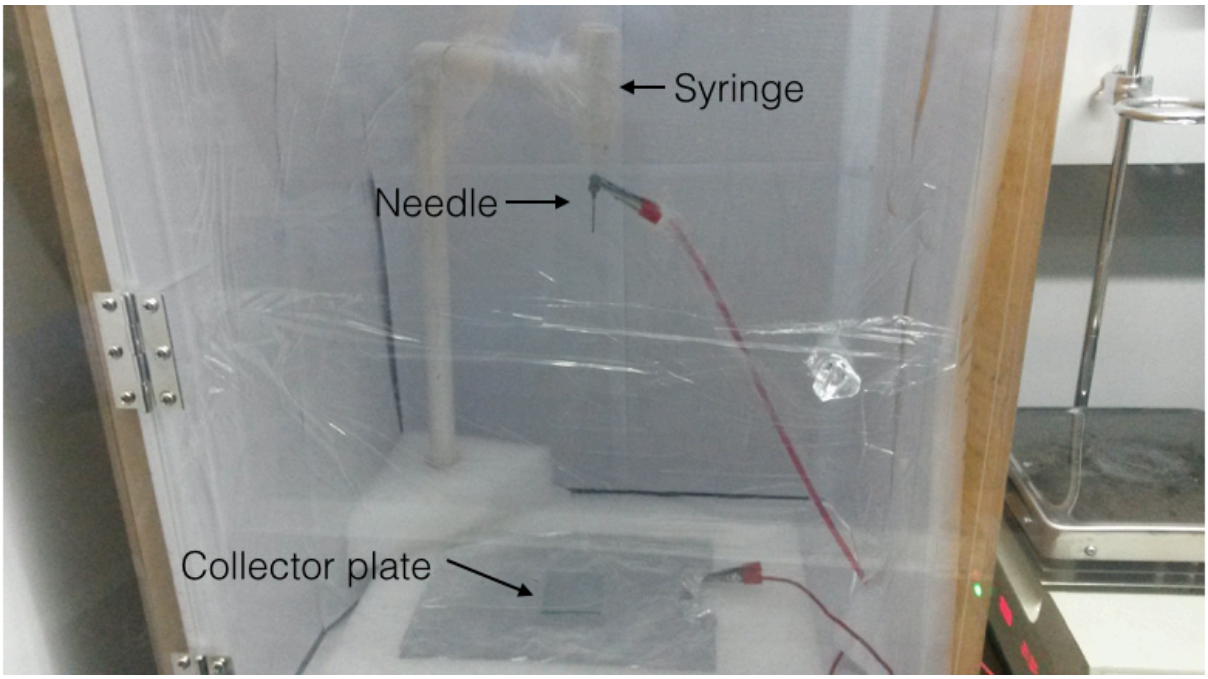

Figure 14 depict the setup for elettrospinning with the syringe, needle, collector plates and the two electrodes.

To conduct the electrospinning, 3 ml of the slurries were fed into the syringe, which was then put into the white syringe stand visualized in figure 14. The electrodes were then connected to the needle and the aluminium foil. After this the high voltage power supply was turned on and

slowly increased to provide 20 kV. The voltage was supplied for 20 minutes to ensure that enough fibres were collected on the collector plate. The fibres were then examined with microscope to ensure that the quality was adequate. Normally the collector plate made of glass would not be suitable for being put in a furnace but because the sintering temperature was kept relatively low there was no inconvenience in using a glass collector plate.

Figure 15 showing the high voltage power supply during operation.

Note! *Successful fibres were only retrieved for the 30- and 40 wt% NiO mixtures due to the limited amount of time.*

3.4 Sintering

After the fibres had been produced, they were sintered in a furnace. The sintering process is done to fuse to particles together and to get rid of impurities. It is a kind of calcination process that is needed for the fibres not to be vanished. The temperature that was used for the sintering was 400°C for the 30 wt% NiO fibres and 400, 450 and 500°C for the 40 wt% NiO fibres and the time spent in the furnace was 2 hours.

3.5 Remaining parts of the project

The shortage of time in China meant that some of the experimental steps had to be omitted from this thesis. These are only described shallowly.

3.5.1 Ni-coating

The Ni-coating is to be done to the pure YSZ-fibres after sintering. It can be done by first sensitizing the fibres by using for example acidified $SnCl_2$ and $PdCl_2$ hydrosols. After drying the fibres in a furnace they can be sunk into a coating solution to deposit the Ni on the YSZ. An example of a Ni-containing used in previos studies (Li, Zhang, Liu, & Guo, 2010) can be found in table 5 below.

Table 5 depicts a possible composition of a solution for Ni-coating.

Substance	Concentration
$Ni(AC)_2$	50 g/L
EDTA	20 g/L
Lactic Acid	40 mL/L
N_2H_4	80 mL/L
NaOH	35 g/L

3.5.2 Electrochemical impedance spectroscopy

The performance of the anode materials can be measured through a variety of methods. One method is to use electrochemical impedance spectroscopy (EIS), which measures the losses of the different cell components. EIS is usually measured through applying an AC potential to a electrochemical cell and then measuring the current through the cell. By applying Ohms law it is possible to determine the cell resistance (Barfod, Hagen, Ramousse, Hendriksen, & Mogensen, 2006). The sum of the resistance of the cell can be written as in equation 3-8.

$$\boldsymbol{R_{measured} = R_{aux} + R_{elec} + R_{cath} + R_{ano} + R_{conc}} \qquad \textbf{Eq. 3-8}$$

R_{aux} is the resistance in the auxiliary layers of the test cell and R_{elec} is the resistance of the electrolyte. R_{conc} is the diffusion and conversion losses at the anode and R_{ano} and R_{cath} are the electrochemical and chemical losses at the anode and cathode, respectively. It can be noted that the last four terms are equal to R_{cell}. Besides the gas diffusion losses, the microstructure of the anode also affects the charge transfer between Ni and YSZ. (Barfod, Hagen, Ramousse, Hendriksen, & Mogensen, 2006).

3.5.3 Porosity test

The porosity of the structure will be evaluated to judge whether the fibres are providing enough space for fuel to flow into the structure. To conduct the porosity test, the fibres are weighed and then sunk into water. The samples are then weighed again and by that it is possible to find out the volume of water occupying the empty spaces in the fibres and hence the porosity is retrieved.

4 Results

As previously mentioned, successful fibres were only obtained from the 30- and 40 wt% NiO slurries due to the limited amount of time spent in China. To characterise these, scanning electron microscope images (SEM-images) where taken. The result chapter depicts the SEM-pictures of the two different fibre compositions. For the 30 wt% NiO only one sintering temperature was used but for the 40 wt% NiO three different sintering temperatures were used. It should be noted that it is not necessarily the same sample shown for the pre-sintered and the sintered fibres since multiple collector plates were covered in YSZ-NiO films. Hence, the apparent large difference in density between the 40 wt% pre-sintered and sintered fibres are of minor importance.

4.1 30 wt% NiO pre-sintered sample

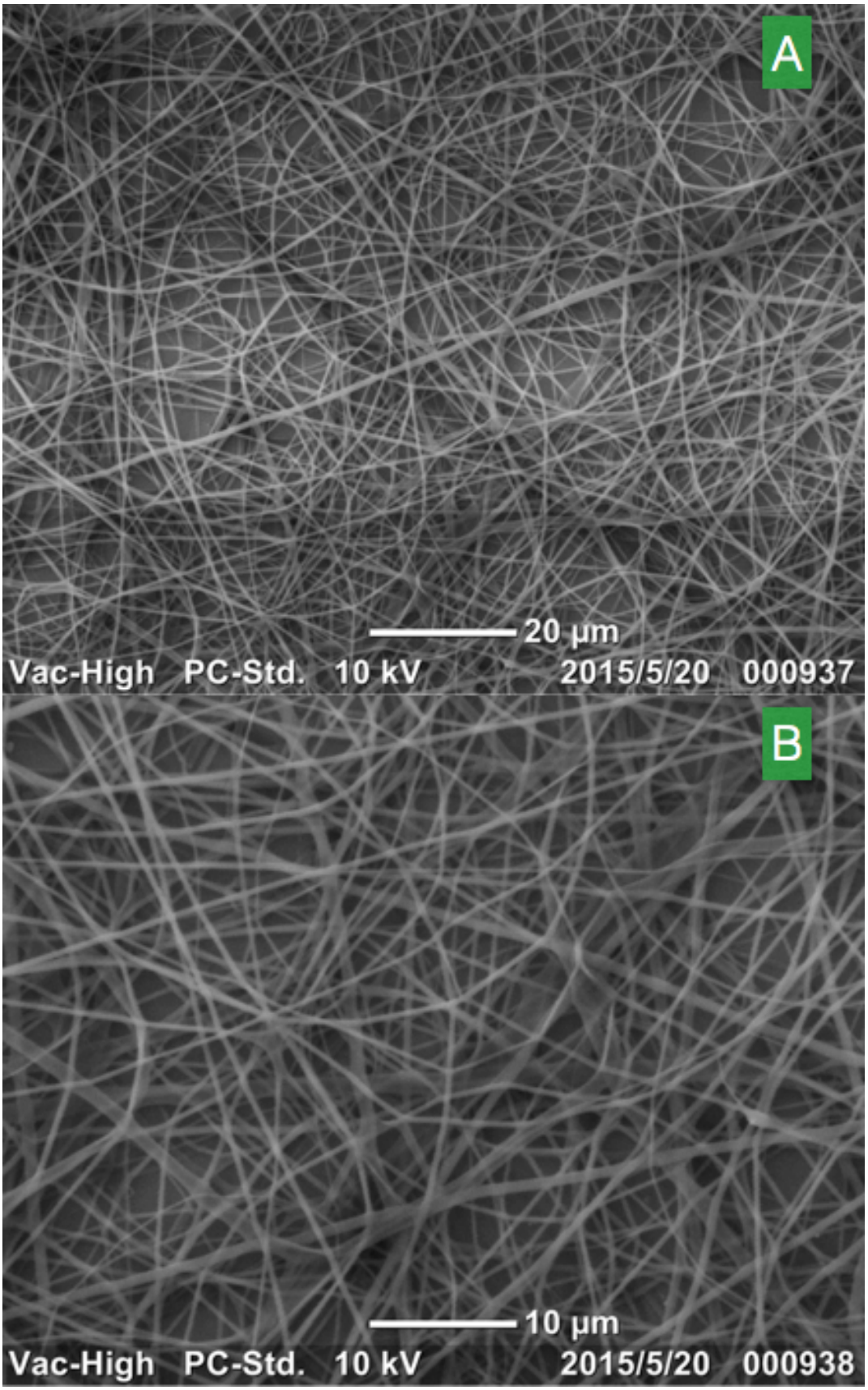

Figure 16 depicts the pre-sintered fibres with 30 wt% NiO at different magnifications.

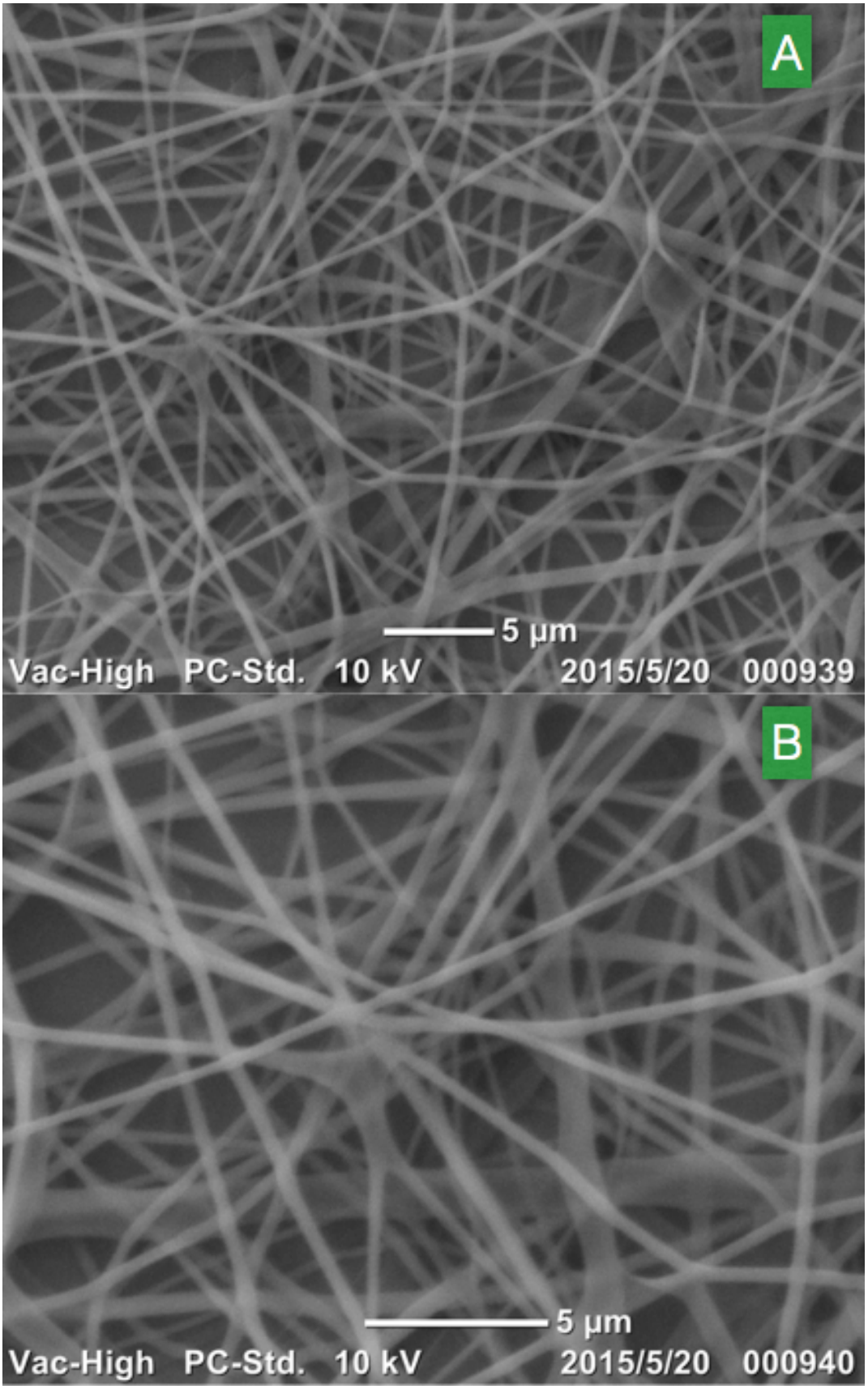

Figure 17 shows the pre-sintered fibres with 30 wt% NiO at different magnifications.

Figure 16 and 17 show SEM-images with different magnifications of the pre-sintered fibres with 30 wt% NiO. A dense, thin network of fibres was created by the electrospinning. Some small droplets were deposited on the collector surface during the electrospinning, though they are not visible in these images. The fibres fabricated during the start up of the power supply and the shutdown usually have a thinner diameter, however this is not visible here since there are so many layers of fibre that it is not possible to distinguish the earlier layers and the later ones.

4.2 30 wt% NiO sintered (400°C) sample

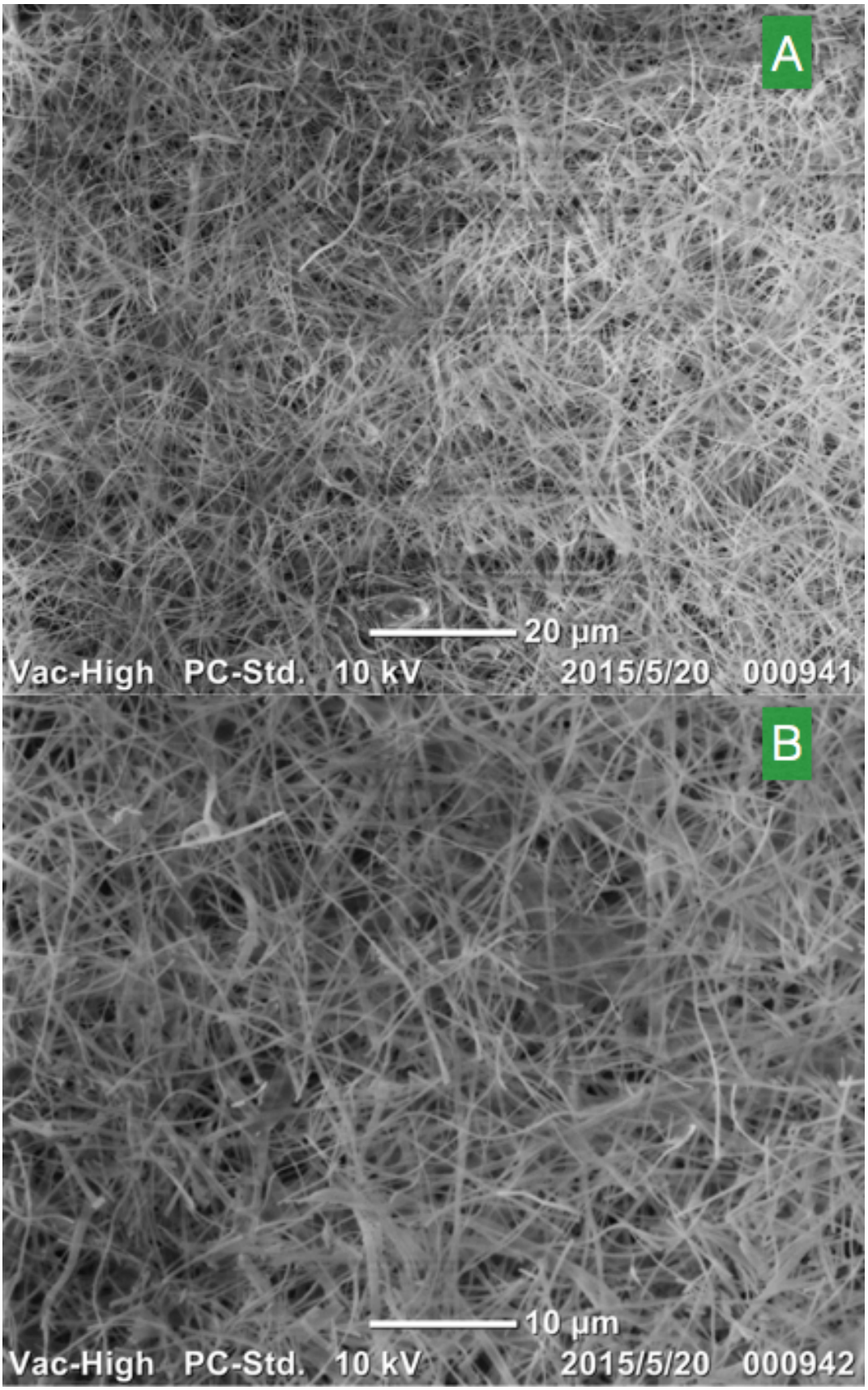

Figur 18 depicts sintered fibres with 30 wt% NiO at different amplifications.

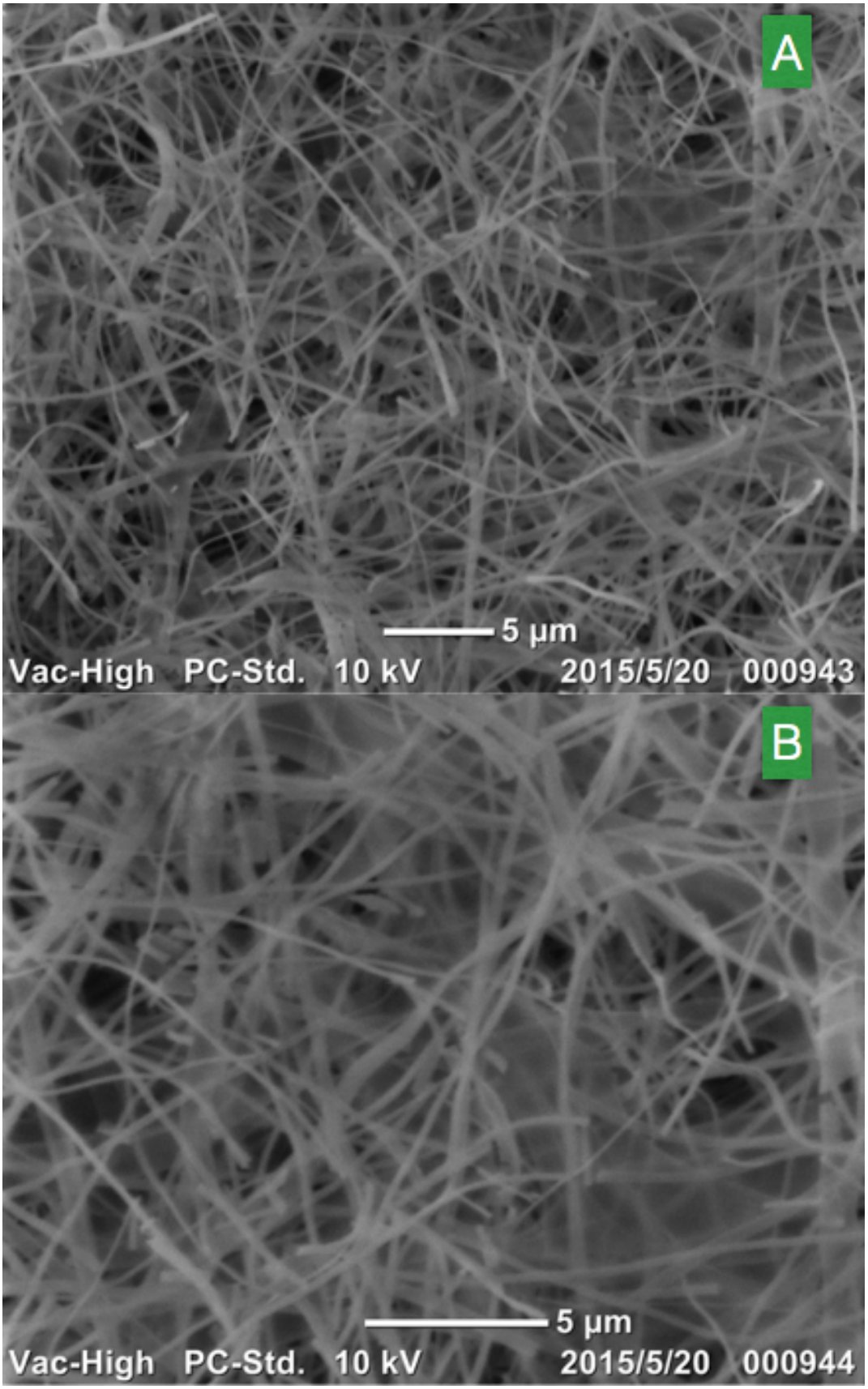

Figure 19 shows the sintered fibres with 30 wt% NiO at different magnifications.

Figure 18 and 19 depict SEM-images with different magnifications of the fibres with 30 wt% NiO sintered at 400°C. The fibre structure of the 30 wt% NiO fibres sintered at 400°C is more dense than the pre-sintered fibres and have thinner diameter, which can be seen, especially when comparing figure 19B with figure 17B. The fibre film shrunk in the furnace and formed a small flake on the collector surface. The flake appeared to have gained some small black spots after the sintering. Compared to the pre-sintered fibres the sintered fibres were much more detached from the collector plate and were easily folded.

4.3 40 wt% NiO pre-sintered sample

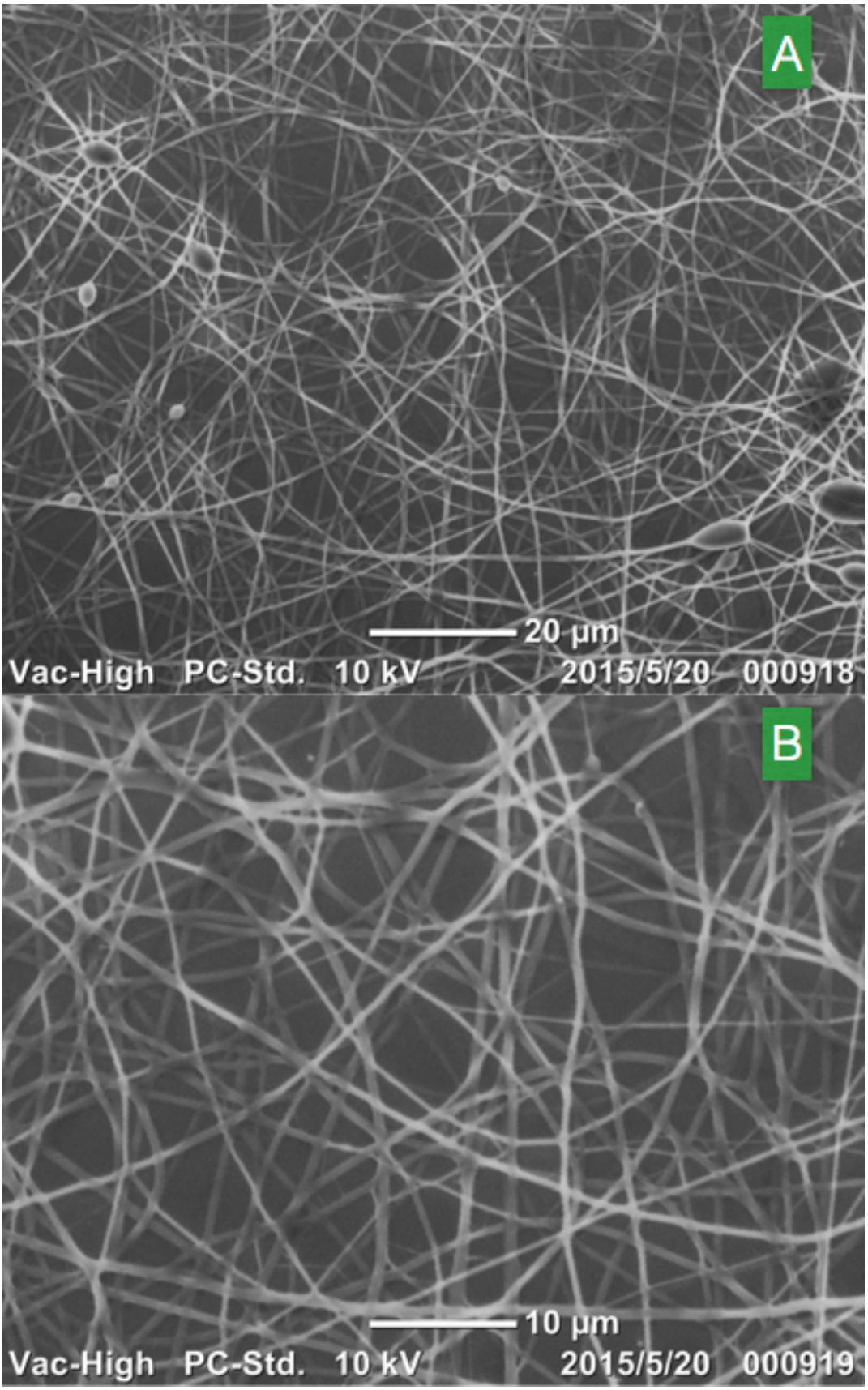

Figure 20 depicts the pre-sintered fibres with 40 wt% NiO at different magnifications.

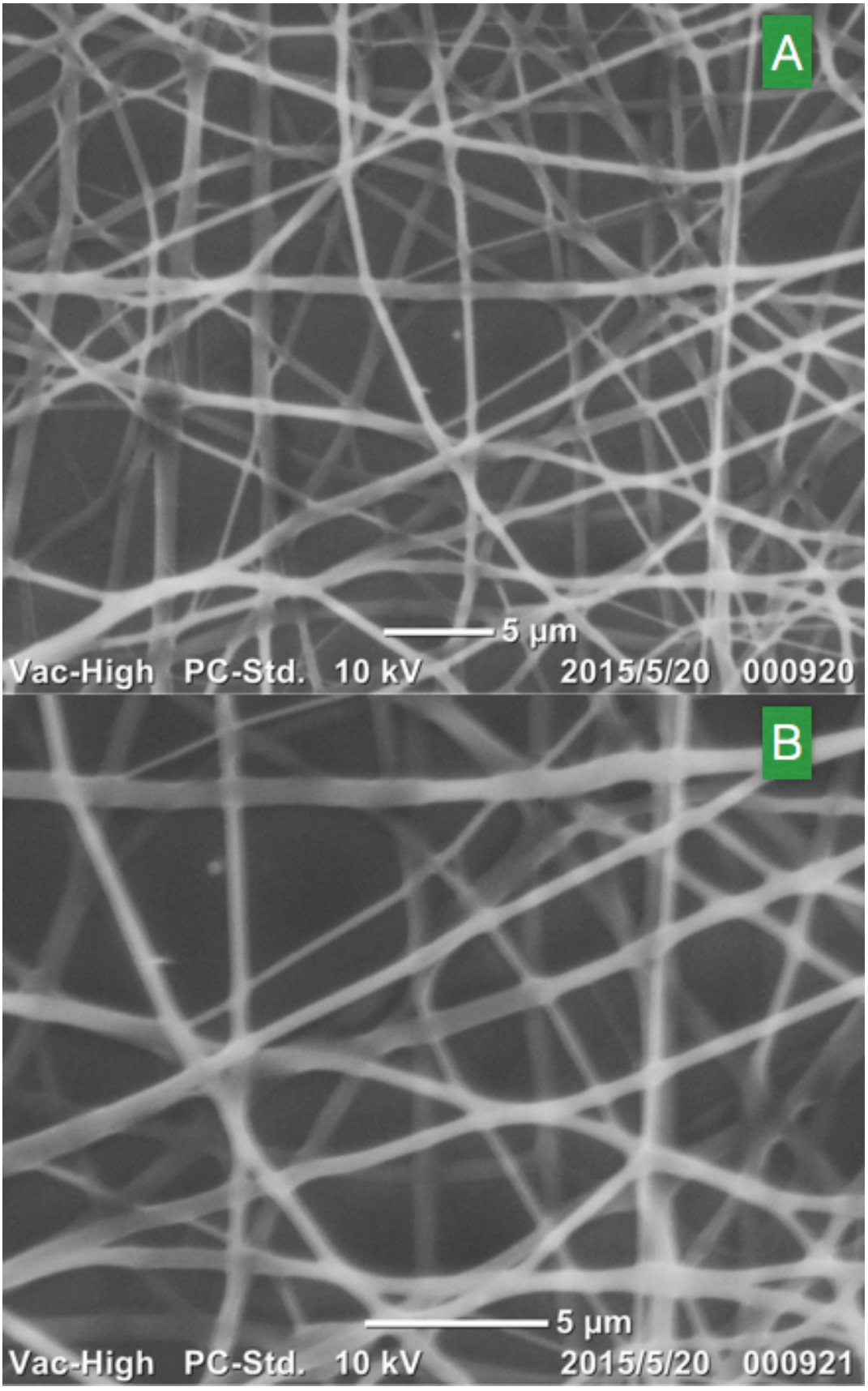

Figure 21 shows the pre-sintered fibres with 40 wt% NiO at different amplifications.

Figure 20 and 21 depict SEM-images with different magnifications of the pre-sintered fibres with 40 wt% NiO. The SEM-images of the 40 wt% NiO pre-sintered fibres clearly shows droplets from the electrospinning. This is shown especially on the right side of the smallest magnification in figure 20A. The fibre structure appears to be less dense than the 30 wt% NiO, however this is dependent on where on the collector plate the image is taken since the film is not a uniform layer. The thickness of these fibres was of the same magnitude as the pre-sintered fibres of the 30 wt% NiO sample.

4.4 40 wt% NiO sintered (400°C) sample

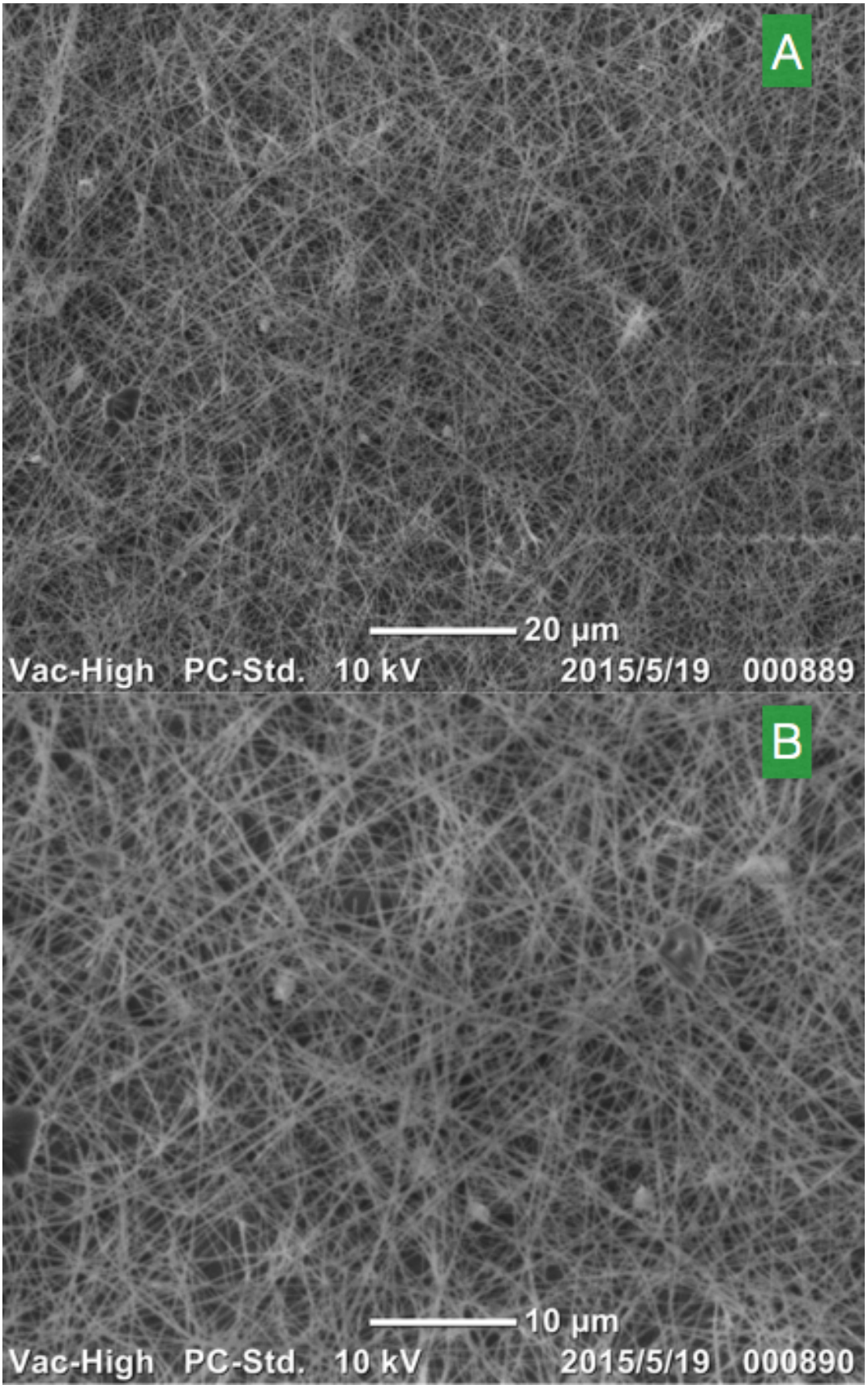

Figure 22 depicts the fibres with 40 wt% NiO sintered at 400°C at different magnifications.

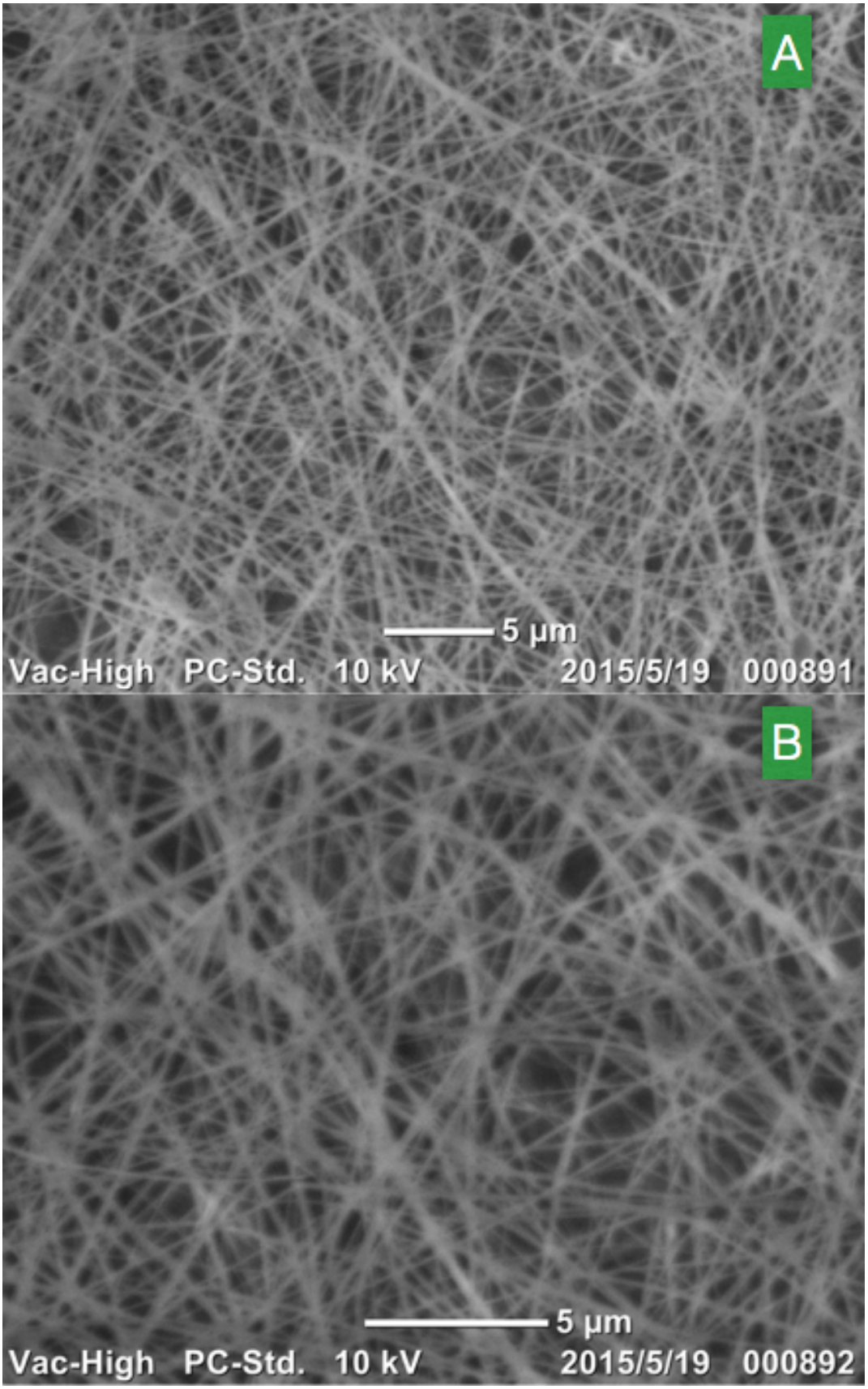

Figure 23 depicts the fibres with 40 wt% NiO sintered at 400°C at different magnifications.

Figure 22 and 23 show SEM-images with different magnifications of the fibres with 40 wt% NiO sintered at 400°C. The fibres of the 40 wt% NiO forms just as for the 30 wt% NiO fibres a more dense structure after being sintered at 400°C compared to the pre-sintered fibres. The two images in figure 22 with least amplification show some presence of agglomerated particles, which might be inherited from the droplets. The structure for this sample seems to have a denser structure than the 30 wt% NiO sample.

4.5 40 wt% NiO sintered (450°C) sample

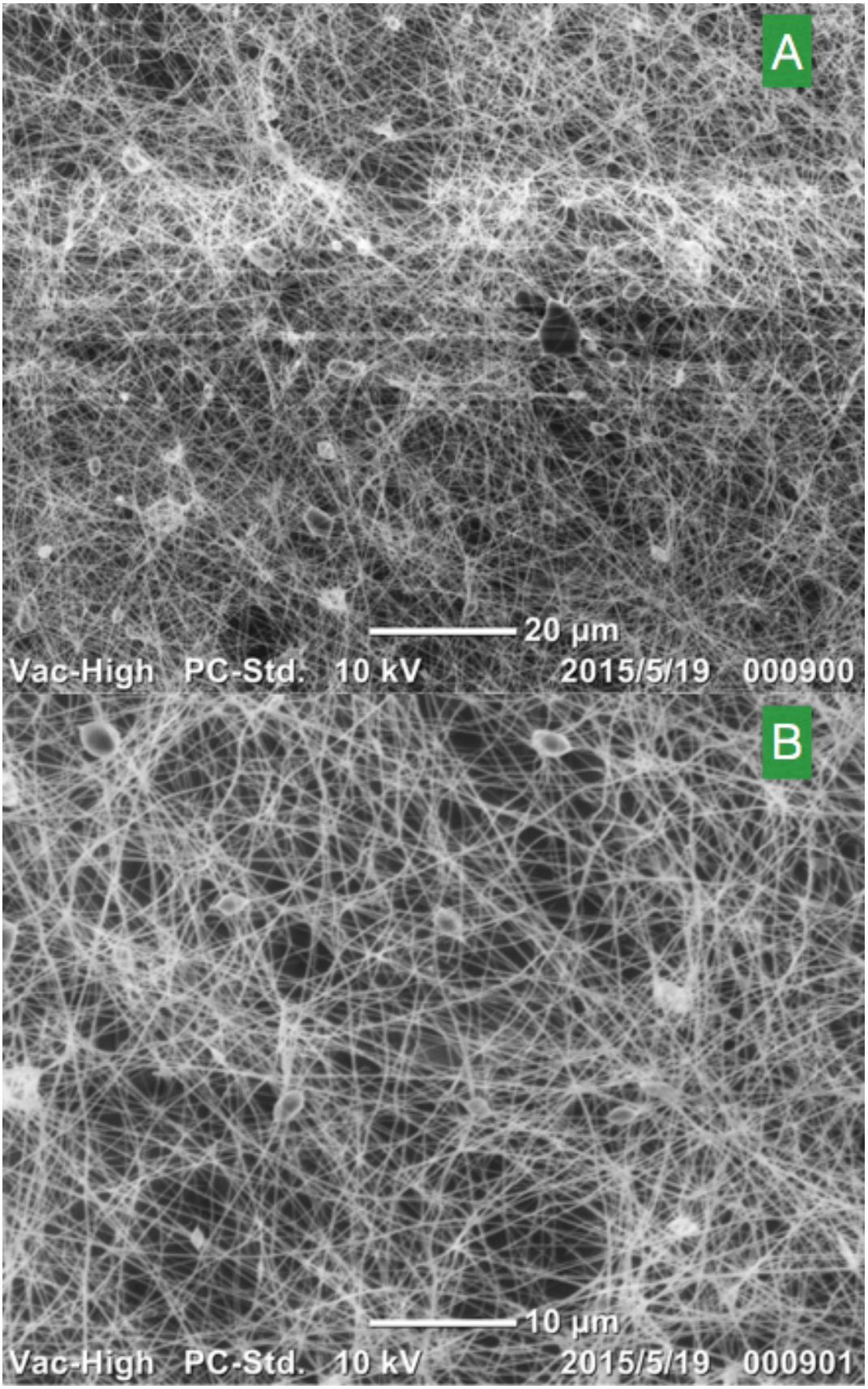

Figure 24 depicts the fibres with 40 wt% NiO sintered at 450°C at different magnifications.

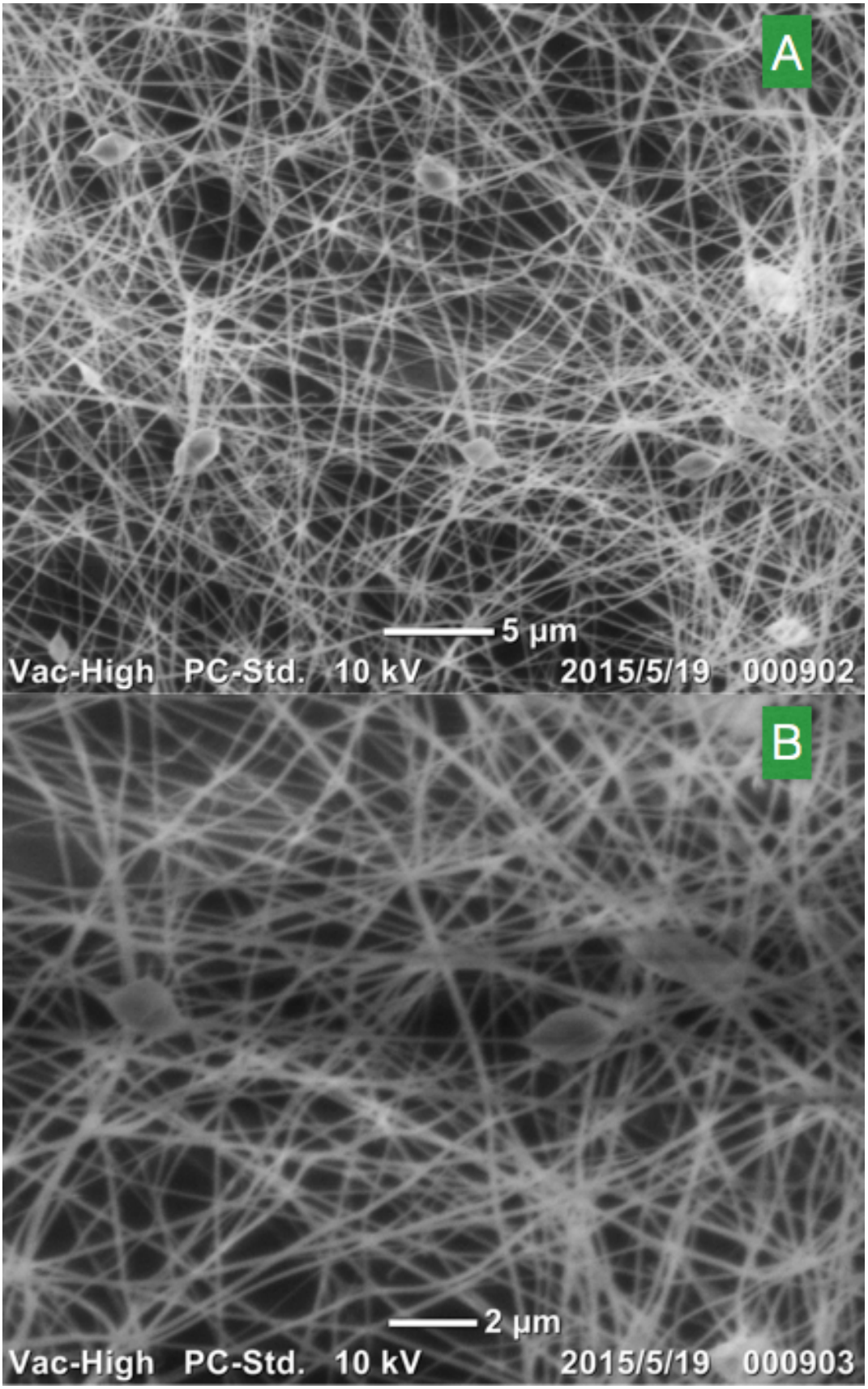

Figure 25 depicts the fibres with 40 wt% NiO sintered at 450°C at different magnifications.

Figure 24 and 25 visualize SEM-images with different magnifications of the fibres with 40 wt% NiO sintered at 450°C. The fibre structure of the fibres sintered at 450°C seems to be more damaged and less dense than the one sintered at 400°C. This was visible not only on a microscopic level, but also by the naked eye when removing the samples from the furnace after the sintering. The traces of the droplets from the electrospinning are clearly shown on all the different magnification levels.

4.6 40 wt% NiO sintered (500°C) sample

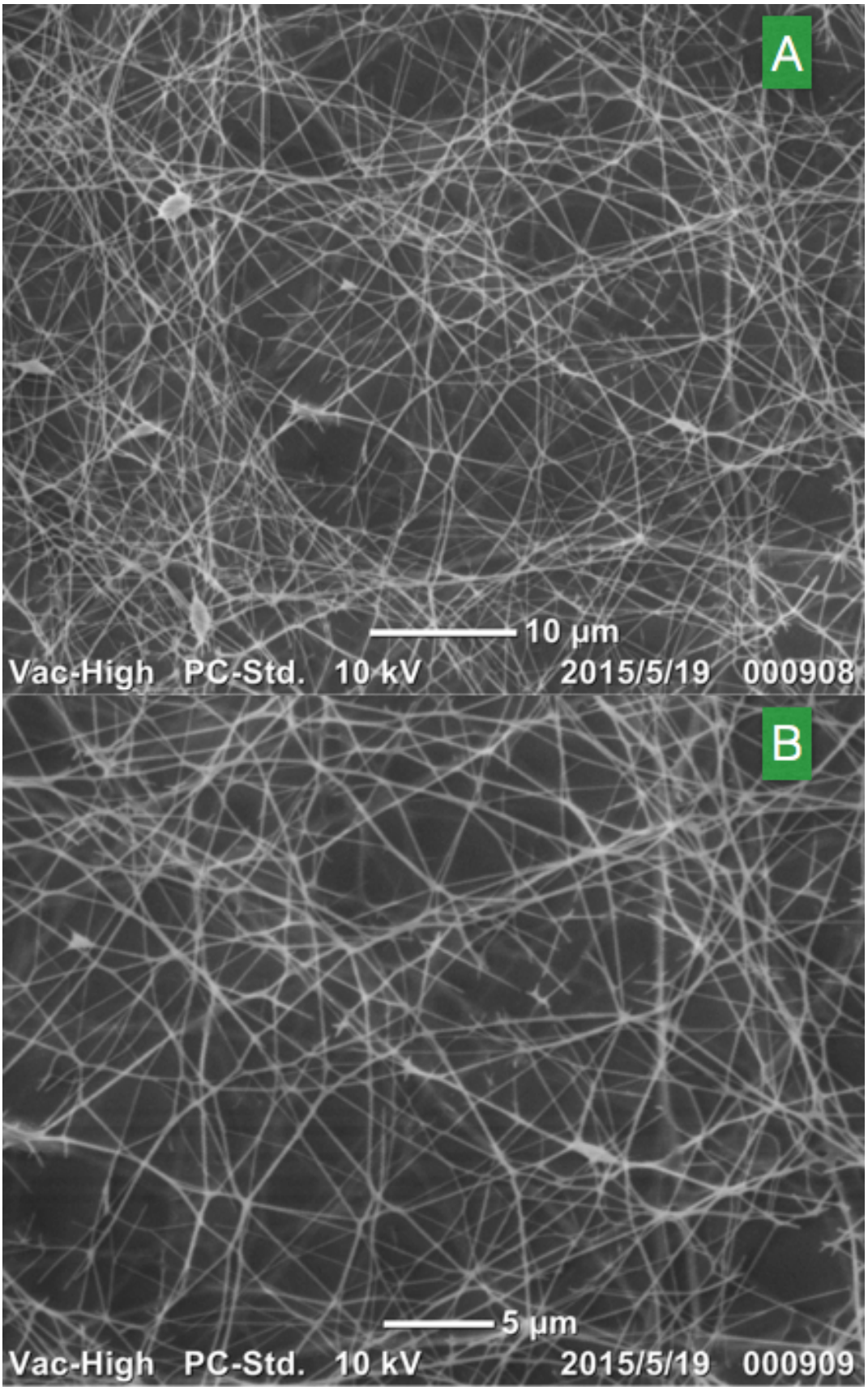

Figure 26 depicts the fibres with 40 wt% NiO sintered at 500°C at different magnifications.

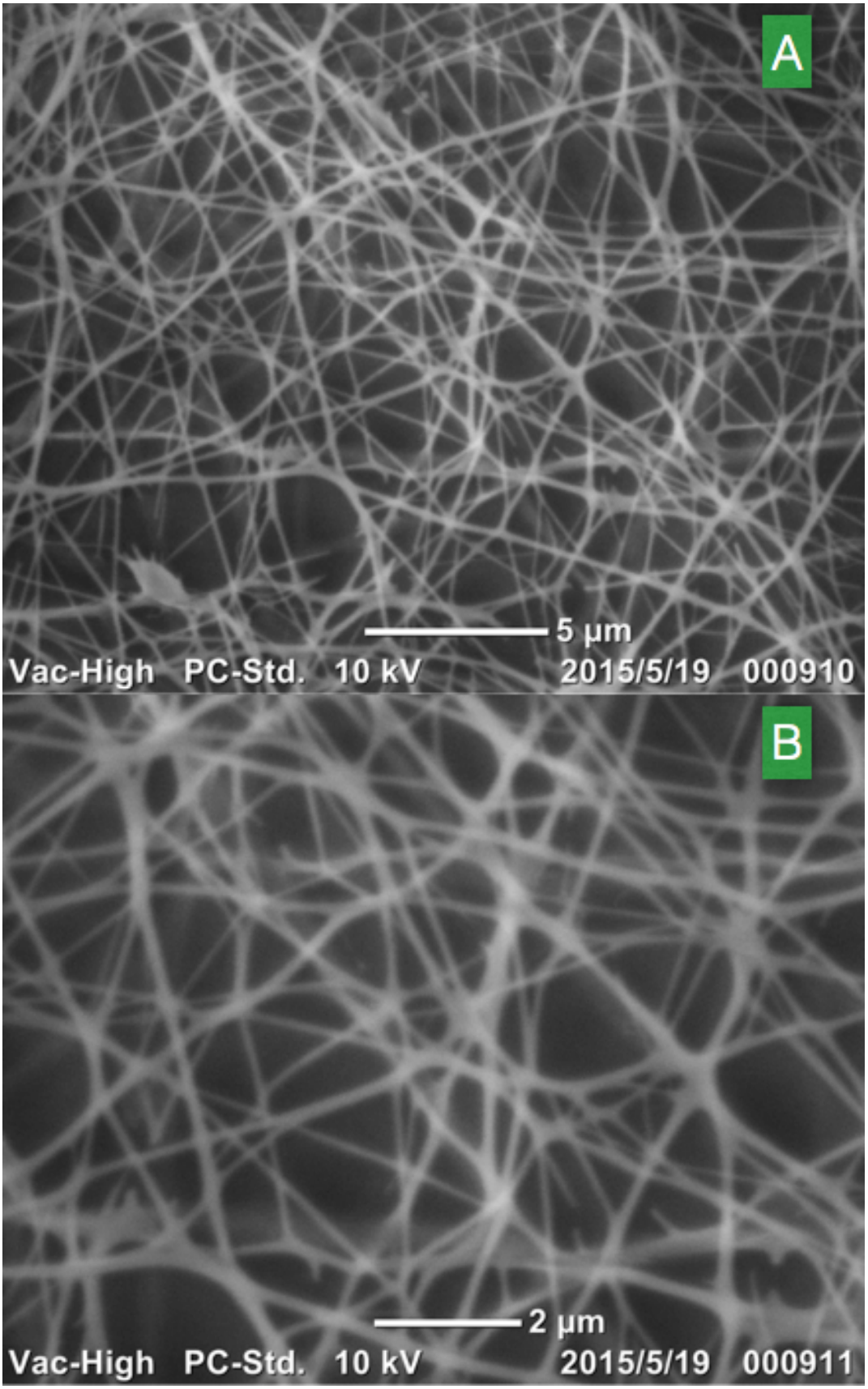

Figure 27 depicts the fibres with 40 wt% NiO sintered at 500°C at different magnifications.

Figure 26 and 27 visualize SEM-images with different magnifications of the fibres with 40 wt% NiO sintered at 500°C. The fibres of the 40 wt% NiO sintered at 500°C are clearly less dense than the fibres sintered at 400°C and 450°C. Just as for the sample sintered at 450°C the flakes of sintered fibres on the collector plates were clearly smaller than the ones sintered at lower temperatures. The structure had a fragile appearance and there are some traces of droplets, especially in all images except 27B, from the electrospinning.

5 Discussion

The discussion chapter is divided into two parts. The first one discusses the fibre structure from the SEM-images and the second part discourses the experimental issues. The discussion chapter omits speculation regarding the evaluation through the impedance spectroscopy and the porosity test.

5.1 The fibre structure

The SEM-images show structures that have the potential to provide lots of TPB:s. The porous structure provides high potential for fuel diffusion and water steam removal. With the electron conductor Ni fused into the fibre structure these structures have the potential of having a high number of TPB:s. However it is very hard to predict the electron conductivity since this is dependent on uninterrupted Ni-chains. Theoretically higher Ni-content should yield a greater potential for the electron conduction. On the other hand, less Ni means that the difference in TEC between YSZ and Ni is less troublesome and should result in a longer lifespan.

Even though the fibre structures survived the sintering process, one big issue remains. The reduction of the NiO when first providing fuel for the anode, which gets rid of the oxygen leads to a significant decrease in volume for the fibres. Since the fibres already are thin and fragile this might lead to breakage of the fibre structure. This might suggest that the fabrication method of NiO-containing fibres is not suitable for this purpose. Another option would be to first mix a slurry for fabricating fibres containing 10 wt% NiO and then add the rest of the NiO through a coating method. The risk of the fibres breaking would decrease by using this method since less NiO make up the structure and the reduction process would cause less volume loss. However, using this method might affect the result of the impedance spectroscopy due to difference in the Ni-structure.

When comparing the fibres with different sintering temperatures it is evident that 500°C leads to too many fibres being annihilated. Hence, a lower sintering temperature is desirable. The problem is that the operating temperature of the cell is higher than this and thusly the fibres might not stand the thermal stress. The different fabrication method mentioned in the second paragraph using only 10% NiO in the slurry might give a better result when sintered at higher temperature since the thermal expansion coefficient of the YSZ and NiO differs. Thus, a lower NiO content would put less stress on the fibre structures when heated.

5.2 Experimental issues

5.2.1 Issues with crystallization

A real time-consuming problem was the issue with crystallization that occurred for the first slurry-mixes. Big lumps of precipitation formed when mixing the four chemicals in ethanol. It

was later concluded that the main issue was the glycine. Glycine is the smallest and most polar amino acid due to the NH_2- and COOH-groups. This means that solvability will increase the more polar the solvent is. Hence, water is a much more suitable solvent than ethanol.

Figure 28 depicts a beaker with rejected slurry due to precipitation. The crystals are shown clearly as white spots on the walls.

The crystallisation issue was very time-consuming and was not solved until mid-April. It also caused a lot of waste of chemicals since multiple slurries had to be thrown away.

5.2.2 Issues with electrospinning

The vertically placed needle caused a lot of dripping problems on the collector plates. This might suggest that the viscosity of the slurries were to low. It was very hard to avoid the drops even though the collector plates were not positioned directly underneath the needle. This problem would have been avoided using the horizontally directed needle, however this kind of setup had other issues, which are discussed later. A try was made to put in a bit of elastic fabric into the syringe, and it stopped the dripping. However it made it difficult for the slurry to pass into the needle.

The result from one of the first attempts for electrospinning was that the viscosity was too high to be able to perform the electrospinning. The needle is very thin and a too high viscosity means that no fluid will spray out of the nozzle. After the extra addition of ethanol the viscosity was decreased and it was possible to get some fluid out of the nozzle. However, the resulting fibres were deemed as a failure.

Figure 29 depicts the slurry with to high viscosity before it was put in the syringe for electrospinning

Another problem that occurred with the electrospinning was that it sometimes was difficult to get a proper film on the collector plate. The process would only yield few fibres in a spread out area on the collector plate. One attempt ended in a fibre structure that reminded of a spider nest structure. Though, it is hard to just blame one factor for the flawed attempt; it could be the distance between needle and collector plate, the viscosity could be wrong etc.

6 Conclusions and further work

The two main objectives of this thesis were first to create four different slurries and then create SOFC anode fibres through electrospinning. The slurry mixing ended up being successful but the time it had consumed meant that there were only room for two different successful fibres to be fabricated. It is hard to draw any clear conclusions before the anode structures have been evaluated by testing conductivity and porosity. However, some things can still be concluded at this stage of the experiment:

- The fabrication method results in a dense fibre structure, but the fibres are very thin and sensitive to the sintering temperature.
- It is desirable to try and prepare slurries with 10% NiO and then coat the fibres in Ni to reach the desired Ni-YSZ ratio. This is the best way to avoid breakage of fibres and it might withstand a higher sintering temperature.
- The sintering temperature must be kept low in order to not destroy the fibres during calcination.
- Droplets can be avoided by better controlling the viscosity and/or by plugging the syringe with absorbing fabric.
- It would be interesting to see if a different way of preparing the slurries could give thicker fibres in the electrospinning.

7 Learning and outcomes

Even though it sounds like a schoolbook cliché it has been a priceless experience to work in a completely new environment. It might seem like the language barrier would be a great hinder and of course, there have been moments when it has, but most of the time it has been smooth sailing. I think it has been a gaining experience communication wise for both my lab partners and me since we have had to practise to express ourselves in new ways. Even though English can be considered to be an almost universal language today it is spoken very differently depending on the native tongue and with an adaption to a more Chinese style of speaking English it was pretty easy to be understood.

Although there are many similarities between an engineering program in Sweden and China it has been the differences that mostly have been catching my attention. The experimental part where long term projects are carried out is something that I feel is missed in the Swedish engineering programs. I think that daily facing the challenge of pushing a project forward in unknown territory can be very useful, especially compared with the schoolbook examples that the Swedish students face mostly in their university years. After graduation in the professional career you are seldom given problems right out of the schoolbook example but instead facing a non-straight path with resemblance of experimental work.

When it comes to the time aspect it is easy to say now but to spend more time in China would probably be a better alternative. 3 months was maybe a too short time to accomplish something giving from an experimental point of view. Another month or two would have provided less stress.

8 Bibliography

Barfod, R., Hagen, A., Ramousse, S., Hendriksen, P. V., & Mogensen, M. (1 February 2006). Break Down of Losses in Thin Electrolyte SOFCs . *Fuel Cells* .

Barfod, R., Mogensen, M., Klemensø, T., Hagen, A., Liu, Y.-L., & Vang Hendriksen, P. (5 Februari 2007). Detailed Characterization of Anode-Supported SOFCs by Impedance Spectroscopy . *Journal of The Electrochemical Society* .

Ceramic Fuel Cells Limited. (19 February 2009). *Ceramic Fuel Cells Limited.* Retrieved from Ceramic Fuel Cells Limited: http://www.cfcl.com.au/Assets/Files/20090219_CFCL_Announcement_60_percent_Efficiency.pdf den 28 May 2015

Chen, Y., Bunch, J., Li, T., Mao, Z., & Chen, F. (16 April 2012). Novel functionally graded acicular electrode for solid oxide cells fabricated by the freeze-tape-casting process . *Journal of Power Sources* , ss. 93-99.

George, R. A., & Bessetteb, N. F. (1998). Reducing the manufacturing cost of tubular SOFC technology. *Journal of Power Sources* , 131-137.

Hoogers, G. (2003). *Fuel Cell Technology Handbook.* Boca Raton: CRC Press.

Kendal, K., & Singhal, S. C. (2003). *High Temperature Solid Oxide Fuel Cells: Fundamentals, Design and Applications.* Oxford: ElsevierLtd.

Kreuer, K.-D. (2013). *Fuel Cells.* New York: Springer.

Kunze, J., Paschos, O., & Stimming, U. (2013). Fuel Cell Comparison to Alternate Technologies. i K.-D. Kreuer, *Fuel Cells* (ss. 77-95). New York: Springer.

Li, D., & Xia, Y. (19 July 2004). Electrospinning of Nanofibers: Reinventing the Wheel? . *Advanced Materials* , ss. 1151-1170.

Li, L., Zhang, P., Liu, R., & Guo, S. (19 August 2010). Preparation of fibrous Ni-coated-YSZ anodes for solid oxide fuel cells. *Journal of Power Sources* , ss. 1242-1247.

Li, T. S., Wang, W. G., He, M., Chen, T., & Xu, C. (1 February 2010). Effect of reduction temperature on the electrochemical properties of a Ni/YSZ anode solid oxide fuel cell. *Journal of Alloys and Compounds* , ss. 138-143.

Li, T., Gao, C., Xu, M., Li, B., Wu, M., & Wang, W. (4 February 2014). Effects of PH3 and CH3Cl Contaminants on the Performance of Solid Oxide Fuel Cells. *Fuel Cells* , ss. 1-7.

Pan, W., Lü, Z., Chen, K., Huanga, X., Wei, B., Li, W., o.a. (2010). Novel polymer fibers prepared by electrospinning for use as the pore-former for the anode of solid oxide fuel cell. *Electrochimica Acta* , 5538–5544.

Suzuki, T., Hasan, Z., Funahashi, Y., Yamaguchi, T., Fujishiro, Y., & Awano, M. (14 August 2009). Impact of Anode Microstructure on Solid Oxide Fuel Cells . *Science* , ss. 852-855.

The Economist. (28 July 2012). Germany's energy transformation Energiewende. *The Economist* .

van den Bossche, M., & McIntosh, S. (2013). Direct Hydrocarbon Solid Oxide Fuel Cells . i K.-D. Kreuer, *Fuel Cells* (ss. 31-76). New York: Springer.

Wongchanapai, S., Iwai, H., Saito, M., & Yoshida, H. (2012). Performance evaluation of a direct-biogas solid oxide fuel cell-micro gas turbine (SOFC-MGT) hybrid combined heat and power (CHP) system . *Journal of Power Sources* , 9-17.

Yokokawa, H., & Horita, T. (2012). Solid Oxide Fuel Cell Materials: Durability, Reliability and Cost. i R. A. Meyers, *Encyclopedia of Sustainability Science and Technology* (ss. 9851-9885). New York: Springer.

Zhao, L., Xie, Z.-p., & Wang, C.-a. (January 2013). Preparation and Characterization of 8mol% Yttria-stabilized ZrO2 (8YSZ) Fibers Prepared by Sol-Gel Method. 144-159.